CO5-1 Volcanic and Tectonic History of Philippine Sea Plate (South of Japan) Revealed by $^{40}Ar/^{39}Ar$ Dating Technique

O. Ishizuka, S. Sekimoto[1], R. Okumura[1], H. Yoshinaga[1], Y. Iinuma[1] andT. Fujii[2]

Geological Survey of Japan, AISandT

[1]*Institute for Integrated Radiation and Nuclear Science, Kyoto University*

[2]*Graduate School of Engineering, Osaka University*

INTRODUCTION: Submarine volcanic rocks are known to give ages different from their true eruption ages in some cases. This is due to the existence of excess ^{40}Ar in the rapidly quenched glass or Ar loss and K remobilization caused by reaction with seawater or hydrothermal fluids. Stepwise-heating analysis in $^{40}Ar/^{39}Ar$ dating is particularly useful for dating submarine volcanics.

Robust tectonic reconstruction of the evolving Philippine Sea Plate for the period immediately before and after subduction initiation at ~52 Ma to form the Izu-Bonin-Mariana (IBM) arc is prerequisite to understand cause of subduction initiation (SI) and test competing hypotheses for SI such as spontaneous or induced nucleation. Understanding of nature and origin of overriding and subducting plates is especially important because plate density is a key parameter controlling SI based on numerical modeling (e.g., Leng and Gurnis 2015). There is increasing evidence that multiple geological events related to changing stress fields took place in and around Philippine Sea plate about the time of SI ~52 Ma (Ishizuka et al., 2011). For our understanding of the early IBM arc system to increase, it is important to understand the pattern and tempo of these geological events, particularly the duration and extent of seafloor spreading in the proto arc associated with SI, and its temporal relationship with spreading in the West Philippine Basin (WPB).

The YK19-07S cruise aimed to investigate origin and age of formation of ocean basins in and around the Daito Ridge group. Especially ocean basins which potentially existed in the period of SI to form the IBM arc were the major targets of this cruise, because ocean crust of these basins might be part of overriding plate when subduction of Pacific plate initiated to form IBM arc. Since gravitational instability between the neighboring plates is supposed to be a critical factor for subduction initiation, it is important to understand characteristics (age, origin, crustal structure) of overriding plate to test hypotheses of subduction initiation. Recovery and characterization of igneous crust of these basins will provide crucial information about the possible basement of the IBM arc and critical constraints to evaluate models for subduction initiation along the Pacific margin. Recent cruises in the Philippine Sea basins recovered basalts from ocean crust along the major tectonic lines such as the Oki-Daito Escarpment and Mindanao Fracture Zone of the West Philippine Basin. These samples were dated by $^{40}Ar/^{39}Ar$ dating method to obtain age of formation of the basins.

EXPERIMENTS: Samples were wrapped in an aluminum foil packet and the packets were piled up in a pure aluminum (99.5% Al) irradiation capsule (9 mm diameter and 30 mm long). The irradiation capsule was partitioned into 3 compartments to minimize the horizontal flux variation across the capsule.

For the experiments described here, around 5 mg of sample was analysed. Only minimum acid leaching was applied to the glass samples, i.e., ultrasonic cleaning with 3M HCl for 10 minutes at room temperature. After this acid treatment, the glass chips were examined under binocular microscope before packed for irradiation.

RESULTS: $^{40}Ar/^{39}Ar$ dating of fresh basalt glasses from YK19-07 cruise returned variable results, with some "disturbed" age spectrum (Fig. 1). This spectrum is characterised by some steps with irregularly older ages among those with relatively constant ages of around 58 Ma. These older steps, however, show consistent Ca/K ratios with other steps. This strongly implies that these steps are not associates with particular minerals or melt inclusion, but possibly represent degassing from bubbles or "gas pockets" which partially preserve mantle-derived Ar. Konrad et al. (2019) reported similar spectrum from stepwise heating analysis of pyroxene crystals.

Presence of Ar inherited from mantle is a critical problem in dating glass samples. We still need more examples of high-precision dating experiments to understand behavior of mantle-derived Ar and its effect on age spectrum.

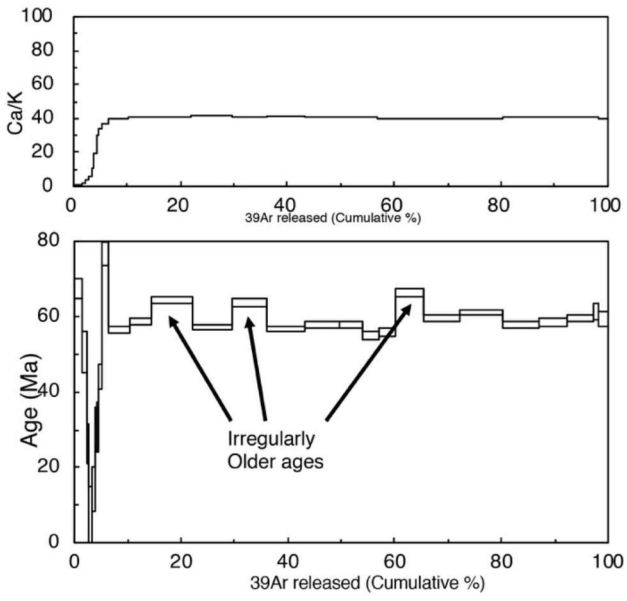

Fig. 1 Age spectrum for the basalt glass from the northernmost West Philippine Basin recovered by submersible Shinkai 6500.

REFERENCES:

[1] O. Ishizuka *et al.* , Earth Planet. Sci. Lett., **306** (2011) 229-240.

CO5-2 Long Term Observation of Element Concentrations in the Atmospheric Aerosols at Sakai, Osaka,1995-2017

N. Ito, A. Mizohata, Y. Iimura[1] and H. Yoshinaga[1]

Radiation Research Center, Osaka Prefecture University,
[1] Institute for Integrated Radiation and Nuclear Science, Kyoto University

Atmospheric aerosols are the fine and coarse particles suspended in the air and are emitted or produced from natural and artificial sources. To investigate the pollution of atmosphere,we have been collecting atmospheric aerosols using particle collector with size separator (Andersen sampler) at Osaka Prefectural University in Sakai City, Osaka since 1994. In this paper we show the some results of long term observations on the element (Cl, V, Cr, Mn, Fe, Zn, As, Br, Sb) which have shown decrease trend. In these element, Antimony (Sb) showed the most remarkable decreasing tendency.

The collection sampler ,Andersen Sampler, has 9 stages on which particle are collected with size ranges (> 11 μm, 7.0-11.0 μm, 4.7-7.0, μm, 3.3-4.7 μm, 2.1-3.3 μm , 1.1-2.1μm, 0.65-1.1μm, 0.43-0.65μm, <0.43μm). By this sampler,atmospheric aerosol was collected on a polyethylene sheet with the collection period of one week.Samples collected on the some part of the sampling perriod were analyzed for the elements by neutron activation analysis using reactors , Rikkyo University, Japan Atomic Energy Agency, and Kyoto University Research Institute for Nuclear Atomic Energy .

To investigate the concentration tendency for 20 year ,we show the size distribution of concentrations in Cl, V, Cr, Mn, Fe, Zn, As, Br, Sb on the two observation periods of 1998 (980203-0210) and 2017 (170328-0404) in Fig. 1. Compared for two periods, the elements that decreased concentration in 2017 for fine particles (<2.1μm) were Cl, Cr, Mn, Zn, and Sb. Concentration change was small for Fe and As.The elements that increased the concentration were V, Br.

The tendency of the concentration change for the fine particles was examined for all observation periods (Fig. 2).Among the analyzed elements, Sb contained in the fine particles (<2.1 μm) showed the most remarkable decrease tendency.The concentration was 0.005 (μg / m^3) at the beginning of the observation (around 1995), but decreased to 0.001 (μg / m^3) in 2017 after 22 years.The slope (a) when approximated by a straight line (ax + b) was -0.25 ± 0.03 (ng / m^3 / year), and the relative increase rate (a / b) was -4.5 ± 0.6 (% / year).Other elements of fine particles were also approximated by ax + b. The estimated range of the increase rate obtained by the range as a ± 2σa indicateing the trend suggest the remarkable decreasing trend for Cl, Cr, Mn, Zn, As, Br, Sb on these elements have the rage of increase as a ± 2σa <0 . Regarding Cr, the tendency of decrease was observed, but the decrease rate was lower than that of other elements. Since fine particles of Cl, Zn, Br, and Sb are included in particles emitted from waste incineration facilities, the reduction of these elements suggests that the effects from waste incineration facilities have been reduced.

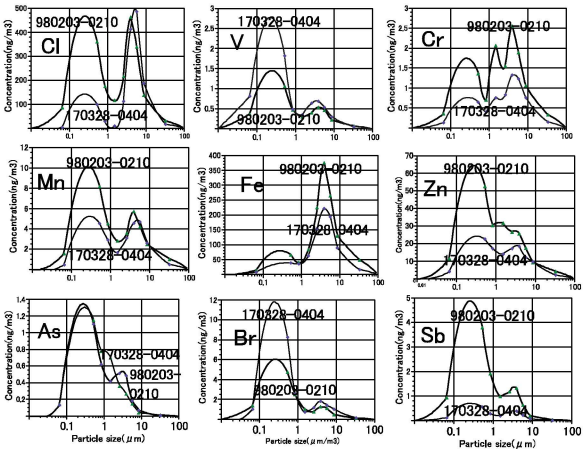

Fig.1. Concentration continuous distributions versus partcle size. The concentratios were obsrved in 980203-0210 and 170328-0404 at Sakai.

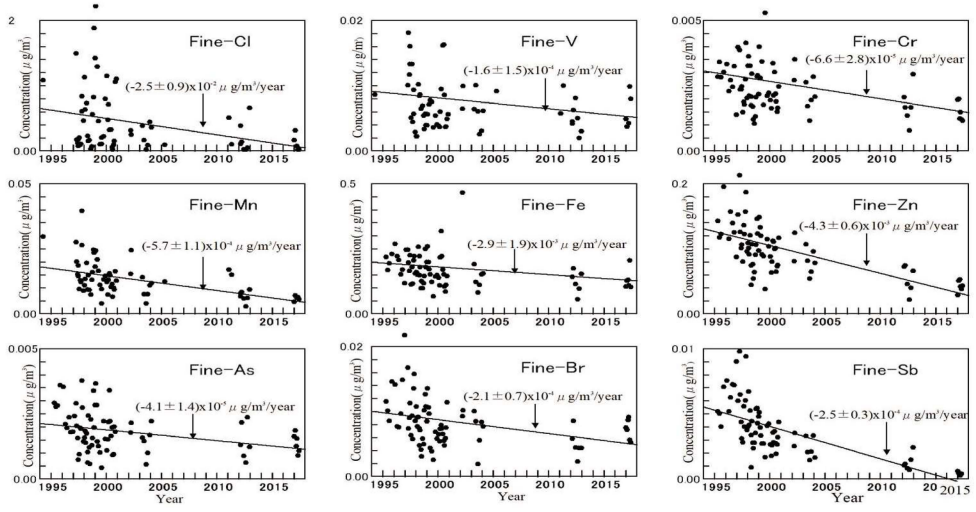

Fig.2. Concentration change in Cl, V, Cr, Mn, Fe, Zn, As, Br and Sb in fine atmospheric aerosols observed at Sakai, 1995-2017. Trends of concentration were estimated by fitting the concentration change with line(ax+b).

31024

Ar-Ar dating of submarine basalts

N. Hirano, H. Sumino[1] and S. Sekimoto[2]

Center for Northeast Asian Studies, Tohoku University
[1] Graduate School of Arts and Sciences, University of Tokyo
[2] Institute for Integrated Radiation and Nuclear Science, Kyoto University

INTRODUCTION: On the western part of the Pacific Plate, most seamounts formed during the Cretaceous pe-riod in the so-called West Pacific Seamount Province (WPSP). The eustatic sea level and global average tem-perature, increasing seafloor spreading rate, and volumi-nous volcanic activities occurred during the mid-Cretaceous period. Many of seamount chains, how-ever, cannot be explained by the classical hotspot and mantle plume hypothesis as well as the Hawaii-Emperor Seamount Chain could be done. Many of seamount and knoll had left their dating behind the volcanic evolutions on the western Pacific Plate. Moreover, the lithospheric flexure-induced volcanoes (petit-spots) are recently de-scribed at the outer-rises of Japan Trench prior to the subduction of northwestern and the western Pacific Plate [1]. Nobody has found such intra-plate volcanoes pre-ceded by the petit-spot volcanic activities since younger WPSP hotspots during Late Cretaceous on the western Pacific Plate. Similar volcanoes have been reported at subduction zones worldwide (e.g., the Japan, Tonga, Chile, and Java trenches) [1][2][3][4][5]. We, therefore, conduct to determine the eruption ages of volcano using Ar-Ar dating to understand the evolution of pacific Plate during Cretaceous to present.

EXPERIMENTS: The research cruise using R/V Yo-kosuka equipped with the submersible SHINKAI 6500, was conducted around the Marcus Island on May 2010 in order to know the detail history during the formation of the Marcus Island (Fig. 1). Radiometric Ar-Ar dating is commonly used to determine the ages of submarine lavas obtained during the submersible dives, because the tradi-tional K-Ar dating is impossible to remove the alteration part of rocks [6]. After the rock-samples, crushed to 100-500 μm grains, they were irradiated by neutrons in a reactor to produce ^{39}Ar from ^{39}K during a few hours. During the irradiation, samples were packed with EB-1 biotite flux monitors [7], K_2SO_4 and CaF_2 as correcting factors in an aluminum capsule. Then, radiogenic ^{40}Ar, daughter nuclide of radioactive ^{40}K and parent, ^{39}Ar in-stead of ^{40}K, were simultaneously analyzed using a mass-spectrometer with an extraction technique of mul-ti-step heating of approximately every 50 to 100 °C be-tween 500 to 1500 °C.

RESULTS: We obtained an estimated eruption age of no more than 3 Ma base on several dating methods of Ar-Ar and others. The NW Pacific petit-spots and this newly described WPSP petit-spot were all erupted from locations in the zone of concave flexure on the outer rise of the lithosphere, prior to its subduction at a trench.

The WPSP eruption site is >1100 km from the Ogasawara Trench and 800 km from the Mariana Trench. These relatively large distances from the trench axes could possibly be explained by the wider outer rise in this subduction system, where the distance to the crest of the outer rise at the Mariana Trench is greater than in other subduction systems [8].

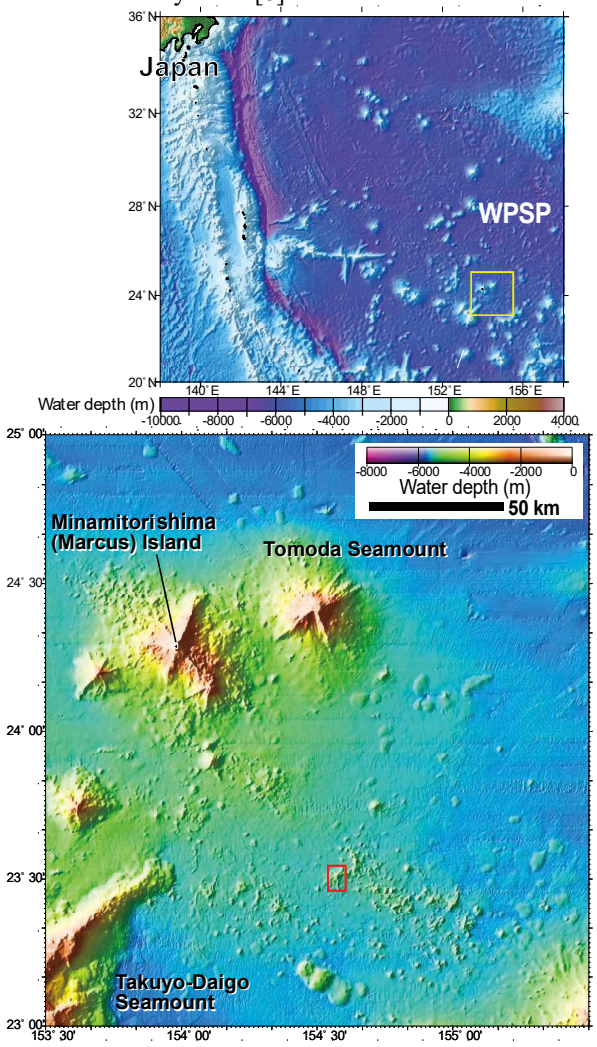

Fig. 1. Bathymetric map of the study area. Yellow box on the upper figure indicate the area of map shown in lower figure. The red square on lower figure indicates the area discovered the young volcano.

REFERENCES:

[1] N. Hirano *et al.*, Science, **313** (2006) 1426-1428.
[2] N. Hirano *et al.*, Basin Res., **20** (2008) 543-553.
[3] N. Hirano *et al.*, Geochem. J., **47** (2013) 249-257.
[4] R. Taneja *et al.*, Gondwana Res., **28** (2014) 391–406.
[5] N. Hirano *et al.*, Marine Geol., **373** (2016) 39–48.
[6] I. McDougall and T. M. Harrison, in *Geochronology and Thermochronology by the $^{40}Ar/^{39}Ar$ Method*, (Oxford, New York, 1988).
[7] N. Iwata, Ph.D. Thesis, Tokyo Univ. (1998).
[8] N. Hirano *et al.*, Deep-Sea Re. I, **154** 103142 (2019).

CO5-4 Recrystallization of an amorphous Si layer by H^+ ion beam and electron beam irradiation

J. Nakata, T. Iha, Y. Hoshino, A. Yabuuchi[1] and A. Kinomura[1]

Department of Math-Phys, Kanagawa University

[1]Institute for Integrated Radiation and Nuclear Science, Kyoto University

INTRODUCTION: IBIEC (ion beam induced epitaxial crystallization) phenomena have been widely studied for about forty years, especially by using MeV ion beam irradiation.[1-3] The author proposed mechanism of IBIEC, consisting of formation of vacant spaces in the amorphous Si (a-Si) layer after vacancy-interstitial recombination in the crystalline Si (c-Si) substrate. The finally remained vacancies after recombination produced at the a-c interface were supplied to the amorphous layer and became vacant spaces in it. These resulted in the vibrational motion of Si atoms wider and more freely, eventually epitaxial recrystallization occurred at lower temperature than that in normal heat treatment. Electron-hole pairs creation also occurred effectively due to MeV ion irradiation. When they are recombined, emitted radiation energy also enhanced the vacancy or interstitial migration, eventually recrystallization rate was greatly enhanced.[4] However, the role of inelastic electronic scattering in the IBIEC process has not been necessarily and directly proved. Thus, we tried to make sure the effect of electronic scattering in the IBIEC process. We compared the IBIEC rate by H^+ ion beam with the EBIEC (Electron Induced Epitaxial Crystallization) rate by e-beam.

EXPERIMENTS: 190 keV Si^+ ions were implanted at 50~60℃ with doses of 5, 10, 20, 50, 100×10^{14}/cm^2 for 10 μA beam current, to form damaged and a-Si layers in the c-Si substrates. Then, 1) IBIEC, 2) EBIEC, 3) furnace annealing were undergone to these above obtained damaged and amorphized substrates. The H^+-IBIEC was conducted at 150 keV with 2×10^{16} cm^2 doses for ~3 μA continuous beam current at 400℃ for 23 hours. 2) The EBIEC was conducted at 7.2 MeV with 4.07×10^{19}/cm^2 doses for ~70 μA pulsed electron beam at 400℃ for 46 hours. 3) thermal annealing for the as-amorphized sample was conducted at 400℃ for 23 hours in vacuum chamber, and for 46 hours in the gold-furnace during Ar ambient flowing. The thicknesses of a-Si layers of these three samples were measured by the Rutherford Backscattering method with 2 MeV Li^{2+} ions, SSB detector being settled at 120℃ angle to the Li^{2+} beam direction.

RESULTS: Figure 1 and 2 show respectively the RBS spectra after IBIEC (mark○ in Fig. 1) and EBIEC (mark ○ in Fig. 2) to the amorphized samples with 2.0×10^{15} /cm^2 Si doses. We also show in these figures for the as-implanted and annealed samples at 400℃ for 23 hours (mark▲ in Fig. 1) and at 400℃ for 46 hours (mark▼ in Fig. 2). As clearly seen in Fig. 1, IBIEC at 400℃ sample (mark○) was crystallized sharply, compared with that (mark▲) of the 400℃-annealing one in vacuum for 23 hours.

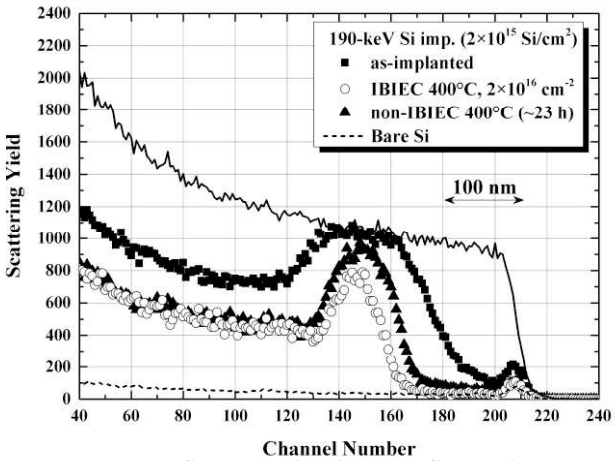

Fig. 1. RBS spectra for the IBIEC sample

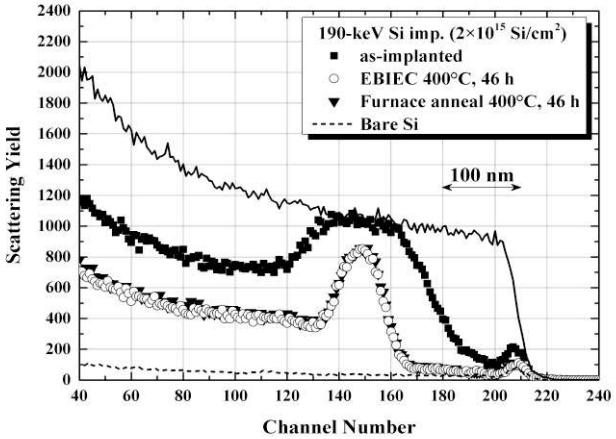

Fig. 2. RBS spectra for the EBIEC sample

As also clearly seen in Fig. 2, EBIEC sample at 400℃ (mark○) was not entirely crystallized at all, compared with that (mark▼) for the furnace-annealed one in Ar ambient at 400℃ for 46 hours.

DISCUSSIONS: In calculation, displaced Si atom density is almost the same for both 150-keV H^+ ion for 2×10^{16} cm^2 and 7.2-MeV electron for 4.07×10^{19}/cm^2 doses at around the a-c interface region. Furthermore, considering the total doses of H^+ ions and electrons, total inelastic electronic deposited energy density in EBIEC is about only 8 times higher than that in IBIEC in spite of the 2000 times higher doses in EBIEC. Consequently, it seems that the IBIEC rate is mainly determined by the elastic energy deposition and it cannot be decisively concluded that the electronic deposited energy density enhances the crystallization rate. It should be noted that IBIEC rate generally decreases as the irradiation dose rate increases. Thus, we should thoroughly compare the dose rate of EBIEC by **pulsed** electron beam with the dose rate of IBIEC by **continuous** H^+ ion beam.

REFERENCES:

1) J. Nakata and K. Kajiyama: Appl.Phys.Lett., **40**(8) (1982) 686-688.
2) J. Nakata and K. Kajiyama: Jpn. J. Appl. Phys., **21** (1982) 211-216.
3) J. Nakata: Phys. Rev., **B43** (1991) 14643-14668.
4) J. Nakata: J. Appl. Phys., **79** (1996) 682-698.

CO5-5 Study on Elemental Concentration in the Atmospheric Particulate Matter by INAA

N. Hagura[1, 2], Y. Okada[2], H. Matsuura[1, 2], T. Uchiyama[2]

[1] Nuclear Safety Engineering, Tokyo City University
[2] Atomic Energy Research Laboratory, Tokyo City University

INTRODUCTION: The Atomic Energy Research Laboratory of Tokyo City University (TCU-AERL) has operated the research reactor "Musashi Institute of Technology Research Reactor (MITRR)" from 1963 to 1989, and has performed various neutron experimental research that is including instrumental neutron activation analysis (INAA). In 2003, it officially decided to decommission the research reactor, and it is currently in the decommissioning stage. At present, all the fuel has been carried out, and it is in the phase of storing and managing radioactive compounds.
Since 2002, sampling of airborne particulate matter have been performed on our facility. Even before that, research on the measurement of radioactivity in the environment has been conducted mainly by Dr. Honda, deceased in 2014, and the concentration distribution of Be-7 and Pb-210 and chemical form in deposition have been analyzed [1]. These studies mainly focused on the behaviors of yellow sand that came to the Japanese archipelago.
After the accident in Fukushima in March 2011, studies on the dynamics of radioactive cesium have been conducted. Especially, focusing on the difference between the rapid decay of radioactive cesium concentration after the accident and the gradual decay after several months, we have been investigating the relationship between the different chemical forms [2, 3].
The sampled filters have been accumulated in the laboratory and are ready to be analyzed again. This fiscal year, we aimed to detect the elements other than cesium by neutron activation analysis, targeting the samples from February to July in 2011.

EXPERIMENTS: We use a high volume air sampler (Shibata Scientific Technology LTD., HV-1000F, filter: ADVANTEC, QR-100 (collection efficiency: 99.99% for 0.3 μm particles)) with an inhalation flow rate of 700 L min^{-1}. Samples are collected approximately every week. The radioactivity of the filter that has collected dust is measured by a high-purity germanium semiconductor detector (ORTEC, GMX-15190-P, wide range energy type, relative counting efficiency: 20.1%, FWHM: 1.22keV at 122keV, 1.9keV at 1.33MeV, wave height discriminator: SEIKO EG&G, MCA-7700), and a part of the filter was stored for neutron activation analysis.
Irradiation was performed at the research reactor KUR at the Institute for Integrated Radiation and Nuclear Science, Kyoto University, between the October and January with four machine times in FY2019. The irradiation conditions are shown in Table 1. The measurement of radioactivity of short half-life nuclides was carried out using the HP-Ge semiconductor detector of the hot laboratory of KUR. And long and medium-lived nuclides, after cooling for one or two weeks, transported to the TCU-AERL, and was measured by a HP-Ge semiconductor detector. JLk-1 was used as a comparative standard substance.

RESULTS: Figure 1 shows the time-series distribution of elements for each sample. Figure 2 shows the correlation coefficients of these 10 nuclides. As expected, we obtained reasonable results of relatively high concentrations of Na, Al, Ca, and Fe. Regarding the correlation coefficient, it was shown that Al and Ca are relatively strongly correlated with other elements.
In the future, we plan to proceed with the analysis of a large number of samples in combination with the PIXE analysis method using the tandem accelerator at our facility (TCU-Tandem) [4], because it is impractical to analyze all samples by the INAA method.

Table 1. Irradiation conditions.

Irradiation			Operating power	Thermal neutron flux
date	time	position		
2019/10/1	30 sec	Pn-3	1 MW	4.7 x 10^{12} n/cm^2/sec
2019/10/23	60 min	Pn-2		5.5 x 10^{12} n/cm^2/sec
2019/12/3	30 sec	Pn-3		4.7 x 10^{12} n/cm^2/sec
2020/1/15	60 min	Pn-2		5.5 x 10^{12} n/cm^2/sec

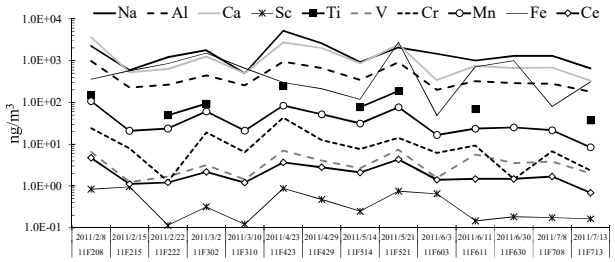

Fig. 1. Transition of element concentration for each sample from February to July in 2011

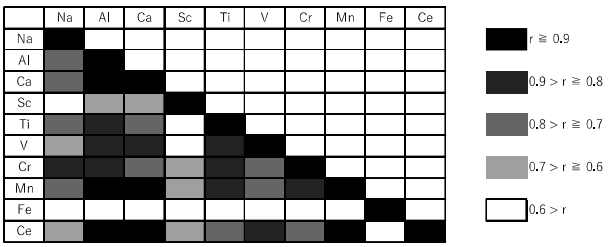

Fig. 2. Distribution chart of correlation coefficient between elements

REFERENCES:

[1] K. Hirose, *et al.*, Atmospheric Environment, 38 (38), pp. 6601-6608 (2004).
[2] K. Nakamachi, *et al.*, Bunseki Kagaku, 64 (8) pp. 589-594 (2015).
[3] N. Hagura, *et al.*, Bunseki Kagaku, 66 (3), pp. 201-204 (2017).
[4] N. Hagura, et al., Transactions of the Atomic Energy Society of Japan, 17 (3-4), pp. 111-117 (2018).

CO5-6 Neutron activation analysis for sediments, phytoplankton, lake water of Lake Akagi Onuma

Y. Okada , T. Uchiyama , N. Kumagai [1], N. Hagura [2], H. Matsuura [2] and Y Iinuma [3]

Atomic Energy Research Laboratory, Tokyo City University

[1]Cooperative major in Nuclear Energy, Tokyo City University

[2]Department of Nuclear Safety Engineering, Tokyo City University

[3]Institute for Integrated Radiation and Nuclear Science, Kyoto University

INTRODUCTION: Contamination of radioactive Cs of Lake Akagi Onuma in Gunma Prefecture was observed due to the accident at Fukushima Daiichi Nuclear Power Station. Recently, the levels of radioactive Cs in wakasagi that live there have been slowly decreasing with the decrease of that of the lake water. In order to clarify the cause of the gradual collapse, we have been investigating the inhabiting organisms and their surrounding areas for 8 years 1, 2).
This study will be conducted as part of investigating the contribution of sediments to lake water. In this research, we investigated lake sediments, phytoplankton, and trace elements in lake water.

EXPERIMENTS: The sediment sample was processed as in the 2018 report. 22 sediment samples from 10 to 570 mm deep collected in 2015, dried phytoplankton, and freeze-dried lake water collected at depths 0, 8 and 15 m in 2018 (wet weight approx. 500 g) was used for the analysis. These samples were double-packed in a clean polyethylene bag. 31 samples (about 50 mg) and comparative standards (JLK1-1, NIES8) were irradiated with a thermal neutron flux of 4.68 × 10 <sup> 12 </ sup> n cm <sup> -for a short time (30 seconds). Neutron flux 5.5 × 10 <sup> 12 </ sup> n cm <sup> -2 </ sup at 2 </ sup> s <sup> -1 </ sup>, long time (3600 s)> KUR s <sup> -1 </ sup>. To monitor neutron flux, approximately 9 mg of aluminum wire containing 1.5% Sb and approximately 11 mg of Fe wire were doubly packed in a clean polyethylene bag and the sample and comparative standard were irradiated together.

The irradiated samples were measured by conventional [γ]-ray spectrometry using a coaxial Ge detector. Analysis of [γ]-ray spectrometry were at Gamma Studio (SEIKO EG&G Co.,LTD).

RESULTS: Using neutron activation analysis, 30 elements in sediment, 19 elements in phytoplankton, and 17 elements in lake water were quantified. Fig. 1 shows the stable Cs concentration in each sediment. The stable Cs concentration changes in the range of 2 μg / g to 5 μg / g at a depth of 10 mm to 570 mm. Among the 19 elements of phytoplankton, it was found that Mg, Mn, Si, Sb and Cs have similar concentrations to those of sediments. Fig. 2 shows a comparison of sediment and phytoplankton smples with Mg, Mn, Si, Rb, Sb and Cs concentrations.

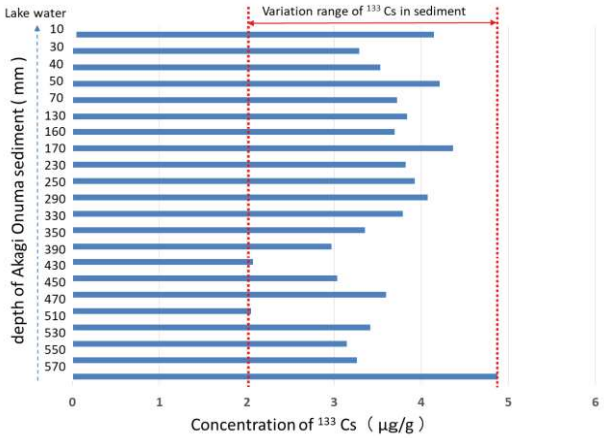

Fig.1 Concentration of ^{133}Cs for each depth of Akagi Onuma sediment

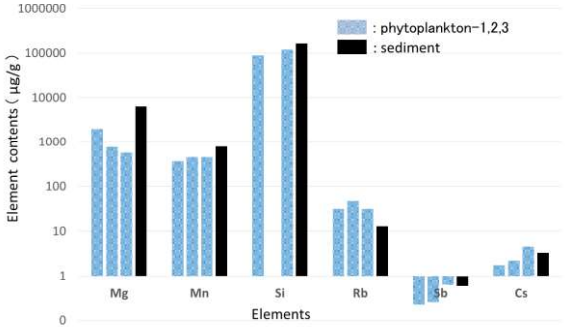

Fig.2 Mg,Mn,Si,Sb,Cs contained in phytoplankton and sediment

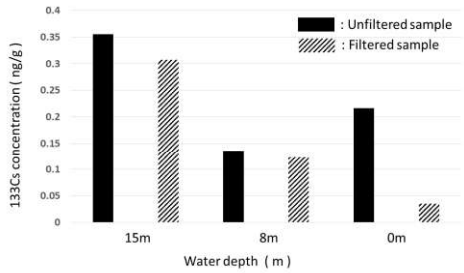

Fig.3 ^{133}Cs(stable Cs) concentration in the lake water of Akagi Onuma (2018 August)

Fig. 3 shows stable cesium quantification results collected in lake water in August 2018. Stable Cs quantification values for unfiltered and filtered lake water are shown at depths of 15 m, 8 m, and 0 m, respectively.
The stable cesium concentration was highest at 15 m. This was the same trend as the radioactive cesium concentration in August. Comparing stable cesium with and without filtration, both 15 m and 8 m showed similar values. From this result, it is considered that stable cesium exists in a dissolved state. At 0m, stable cesium was found to be low with filtration and in suspension collected by 0.45μm filter.

REFERENCES:

[1]K.Suzuki *et al.*, Science of the Total Environment, **622-623** (2018)1153-1164.
[2] M.Mori *et al.*, Science of the Total Environment, **575** (2017)1247-125.

CO5-7 Formation age of Precambrian metamorphic rocks and thermal history

H. Hyodo[1], K. Sato[1,2,3], H. Kumagai[3]and K. Takamiya[4]
[1] *Institute of Frontier Science and Technology, Okayama University of Science*
[2]*Department of Applied Chemistry and Biochemistry, National Institute of Technology, Fukushima College*
[3] *Submarine Resources Research Center, Japan Agency for Marine-Earth Science and Technology*
[4] *Institute for Integrated Radiation and Nuclear Science, Kyoto University*

INTRODUCTION: Acasta gneiss is known as a part of the oldest crust (ca. 4.0 Ga) by U-Pb zircon SHRIMP dating [1]. The thermal history of the rock seems to be complicated [2] because it shows much younger age (1.9 Ga) in apatite U-Pb method [3].

K-Ar system is more susceptive to external disturbance compared to U-Pb system, and wide range of closure temperature. To elucidate the thermal history, hornblende and biotite samples of Acasta gneiss were dated by $^{40}Ar/^{39}Ar$ method.

EXPERIMENTS: Experimental procedure is the same as described as previous studies on single grain datings. Rock samples were crushed and sieved in #25-100 mesh. After ultrasonic cleaning in distilled water, single mineral grains were handpicked. The mineral grains were irradiated in the KUR for 24 hours at 1 MW. The total neutron flux was monitored by 3gr hornblende age standard [4], [5], which was irradiated in the same sample holder. In the same batch, $CaSi_2$ and $KAlSi_3O_8$ salts were used for interfering isotope correction. A typical J-value was $(5.390 \pm 0.068) \times 10^{-3}$. In stepwise heating experiment, the minerals were heated under defocused argon ion laser beam, and temperature of sub-millimeter grains was measured using infrared thermometer whose spatial resolution is 0.3 mm in diameter with a precision of 5 degrees. In order to achieve a precise temperature control, feedback system between temperature monitoring and laser power control were adopted. Extracted argon isotopes were measured using the custom made mass spectrometer with mass resolution of approximately 400 to separate ^{39}Ar peak from neighboring hydrocarbon peak [5].

RESULTS: One of $^{40}Ar/^{39}Ar$ age spectra of biotite grains were illustrated in Fig. 1. The plateau age 1.935 Ga is consistent with 1.964 Ga of the hornblende and the U/Pb age of apatite of the Acasta gneiss, considering a prolonged thermal history.

The area known to have a metamorphic history caused by

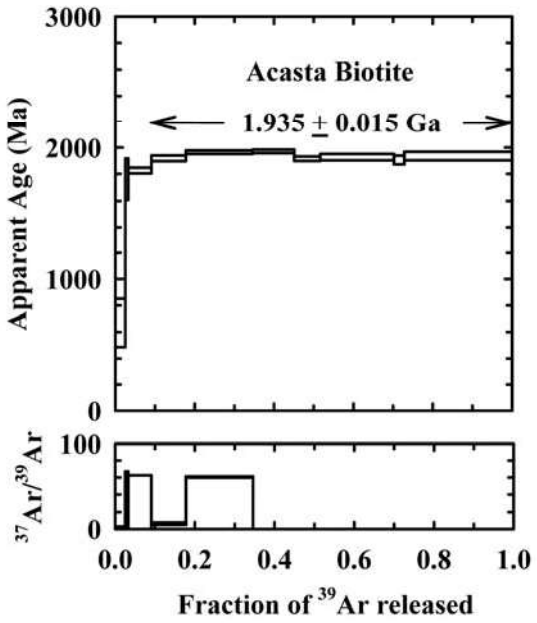

Fig. 1. $^{40}Ar/^{39}Ar$ age spectra of a biotite grain from Acasta gneiss. The $^{37}Ar/^{39}Ar$ error seems to be large, but little effect on the age spectra with a well-defined plateau.

Wopmay orogen around 2.0 Ga. On the other hand, zircons from the area typically show 4.0 Ga. The age gap seem to represents the difference in closure temperature of minerals.

Closure temperature depends on the grain size and cooling rate of the orogen. If we apply typical closure temperatures of hornblende and zircon, The Acasta area was heated to at least above 500°C and below 900°C, and the zircon preserved the formation age, but the hornblende was reset by the Wopmay metamorphism.

REFERENCES:

[1] S.A.Bowring and I.S. Williams, *Contributions to Mineralogy and Petrology*, **134** (1999) 3–16.
[2] T. Iizuka *et al. Precambrian Research* **153** (2007) 179-208.
[3] Y. Sano, *et al., Geochimica Cosmochimica Acta* **63** (1999) 899–905.
[4] J.C. Roddick, *Geochim. Cosmochim. Acta* **47** (1983) 887-898.
[5] H. Hyodo, *Gondwana Research* **14** (2008) 609-616.

CO5-8 A Study on Evaluation of Redox Condition of Tokyo Bay using Redox Sensitive Elements as an Indicator by Means of Instrumental Neutron Activation Analysis

M. Matsuo[1], K. Shozugawa[1], Y. Guan[1], M. Komori[1, 2], R. Okumura[3], Y. Iinuma[3] and K. Takamiya[3]

[1]*Graduate School of Arts and Sciences, The University of Tokyo*
[2] *Yokohama Environmental Science Research Institute*
[3]*Institute for Integrated Radiation and Nuclear Science, Kyoto University*

INTRODUCTION: Hypoxia is water mass that is deficient in dissolved oxygen (DO), often occurs in closed water areas such as the inner bay [1]. In dredged trenches of Tokyo Bay severe hypoxia has been observed in annual summer seasons. The purpose of this study is to clarify the relationship between hypoxia and the sediment environment of dredged trench by chemical analysis of sediments in the vertical direction, assuming that the effect of past hypoxia could be preserved as a difference in concentrations and/or chemical states of elements in the sediments.

To estimate the sedimentary environment related to redox conditions, various elements have been used. For example, Fe and Mn are used because their various chemical states on Eh-pH diagrams have become clear [2]. And U is used for the evaluation of weak reductive conditions because the redox potential of U(VI)/U(IV) is between Mn(IV)/Mn(II) and S(VI)/S(-II) [3]. In this study, concentrations of Fe, Mn, U, Th, and Ce in the sediments were analyzed by instrumental neutron activation analysis (INAA).

EXPERIMENTS: We sampled sediment cores from the dredged trench and non-dredged seabed off Makuhari, Chiba Prefecture in August 2019. All cores were cut in the vertical direction at 2 cm intervals in the laboratory. Then, the samples were desalted by centrifugation with pure water washing three times and dried at 105 ℃.

Approximately 30 mg of sediments were packed in double polyethylene film bags to perform INAA. All samples were irradiated with neutrons at the pneumatic tube, Kyoto University Research Reactor. Three types of gamma-ray measurement were carried out corresponding to half-lives of elements. For analysis of Mn, samples were irradiated for 10 seconds at 1 MW, and then gamma-ray was measured for 600 seconds by Ge detector after 600 seconds cooling. Regarding U, samples were irradiated for 20 minutes at 1 MW, and then gamma-ray was measured for 1400 seconds after 3-4 days cooling. Regarding Fe, Th and Ce, samples were irradiated for 20 minutes at 1 MW, and the measuring time of gamma-ray was for 10000 seconds after 2-3 weeks cooling.

RESULTS: The concentration of Mn was lower in dredged trench than that in non-dredged seabed, suggesting that the dredged trench was in more reductive condition (Fig. 1). On the other hand, there was no significant difference for Fe. It is well-known that the concentrations of both Fe and Mn in sediments increase when condition of seawater is oxidative. However, we note that Mn precipitates under more oxidative conditions. Therefore, it is estimated that the oxidation-reduction potential in the dredged trench remained to the extent that Fe precipitation occurred but no Mn precipitation occurred.

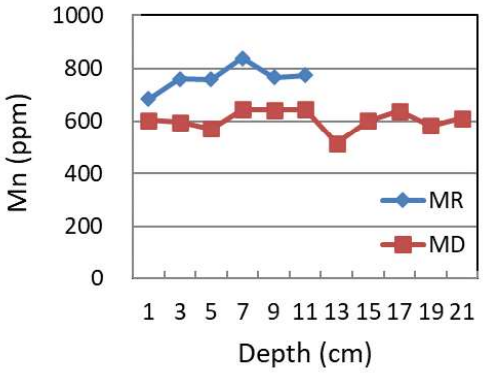

Fig. 1. Depth profile of Mn concentration in the sediments collected from dredged trench (MD) and non-dredged seabed (MR) off Makuhari.

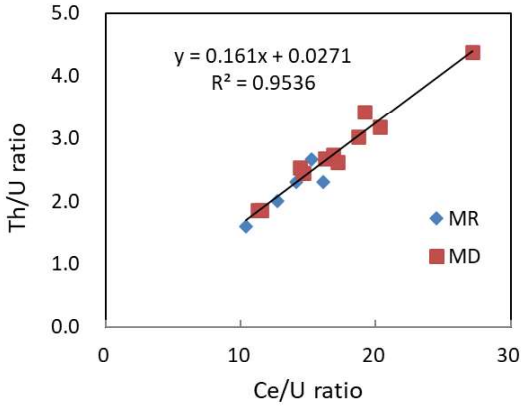

Fig. 2. Th/U-Ce/U plots in the sediments collected from dredged trench (MD) and non-dredged seabed (MR) off Makuhari.

In addition, we plotted the relation between Th/U and Ce/U ratios (Fig. 2). The values of Th/U and Ce/U ratios at each site existed on a same line. This fact indicates that the sediments cannot be the mixture of two or more sources which have different Th/U and Ce/U ratios. However, this figure shows that MD samples are in more oxidative condition. Also, comparing the MD sample ratios with the values of 2017-year sample shows that the dredged trench in this year is more oxidative. This fact indicates that the anoxic state is gradually recovering.

REFERENCES:

[1] R.J. Diaz *et al*., Science, **321** (2008), 926-929.
[2] D.G. Brookins, in *Eh-pH diagrams for geochemistry* (Springer-Verlag, 1988).
[3] D.R. Turner, M. Whitfield and A.G. Dickson, Geochim. Cosmochim. Acta, **45** (1981), 855-881.

CO5-9 Absorption of alkali metal ions by white radish sprouts

M. Yanaga, K. Ogawa[1], T. Nagakura[1], H. Yoshinaga[2], R. Okumura[2] and Y. Iinuma[2]

Center for Radioscience Education and Research, Faculty of Science, Shizuoka University

[1]*Department of Chemistry, Faculty of Science, Shizuoka University*

[2]*Institute for Integrated Radiation and Nuclear Science, Kyoto University*

INTRODUCTION: The Fukushima Daiichi Power Plant accident caused a large amount of radioactive materials released in to the atmosphere[1-3]. Radioactive cesium is especially a problem because of its long half-life. Paddy field soil was also contaminated with radioactive cesium. However, simple removal of contaminated soil would create a vast quantity of radioactive waste. Therefore, separating radioactive cesium from the soil is necessary to prevent damage by rumors and to minimize the quantity of radioactive waste.

Previously, we reported that the absorption of radioactive cesium from artificially contaminated soil into rice plants increased by adding a stable isotope to irrigation water and that the possibility that the cesium atoms added were replaced with radioactive cesium atoms in soil [4, 5]. However, addition of excess amount of stable cesium caused an obstacle to growth of rice plant [6]. Therefore, in this study, we conducted hydroponic culture of white radish sprouts and analyzed trace elements contained in leaves and stems to investigate the behavior of cesium added to the culture solution and the competitive relationship between alkali metals.

EXPERIMENTS: *Materials and Method* Cultivation of white radish sprouts was carried out by adding alkali metal ions, such as potassium ions, rubidium ions and/or cesium ions, to a diluted solution of a commercially obtained culture solution, HYPONeX® (HYPONeX JAPAN CORP.,LTD.).

INAA The samples in polyethylene capsules were irra-diated in Pn-3 for 90 seconds and in Pn-2 for 4 hours, for short and long irradiation, respectively. As comparative standards, the certified NIST Standard Reference Mate-rial 1577b Bovine Liver as well as elemental standard for Cs was used. The γ-ray spectroscopic measurements with an HPGe detector were performed repeatedly for the short-irradiated samples: the first measurements for 120 ─ 900 seconds after decay time of 5 - 15 minutes and the second one for 250 - 1200 seconds after 60 - 150 minutes. The long-irradiated samples were measured for 1 - 24 hours after an adequate cooling time (15 - 60 days).

RESULTS: In order to examine the change in the concentration of cesium ions contained in the leaves, white radish sprouts were cultivated by adding 3.0×10^{-5} mol of cesium ions to the culture solution. When only cesium ions were added to the culture medium, the cesium concentration in the leaves increased with the growth of the white radish sprouts, indicating that cesium ions were absorbed and accumulated in the leaves. Furthermore, as shown in Fig. 1, when grown in a mixed solution with rubidium ions, the cesium concentration in leaves increased. Increasing the concentration of rubidium ions in culture medium increased the cesium concentration in the leaves. This suggests that rubidium ions promoted absorption of cesium ions by plants. However, when the cesium ion concentration in the culture solution was tripled, the leaves discolored and growth disorders were observed. On the other hand, when cesium and potassium ions were added in culture medium, cesium concentration in leaves decreased as the potassium ion concentration in medium increased. This suggests that the presence of potassium ions suppress absorption of cesium ions in plants.

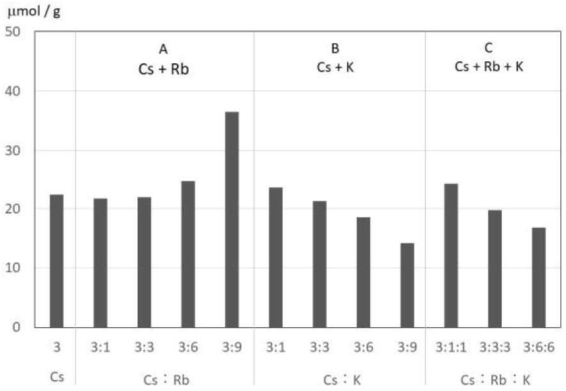

Fig. 1. Cesium ion concentration in leaves of white radish sprouts grown in culture solutions with various alkali metal in concentrations. The amount of cesium ion added to the culture solution was constant and was 3.0×10^{-5} mol.

REFERENCES:

[1] S. Endo *et al.,* J. Environ. Radioact., 111 (2012) 18-27.
[2] M.Yanaga and Y. Oya, Radiation Safety Manage-ment, 12 (2013) 16-21.
[3] M.Yanaga *et al.,* Radiation Safety Management, 12 (2013) 37-42.
[4] M. Yanaga *et al.*, NMCC ANNUAL REPORT, 22 (2015) 185-190.
[5] M. Yanaga *et al.*, NMCC ANNUAL REPORT, 23 (2016) 172-179.
[6] M. Yanaga *et al.*, KURNS Progress Report 2018 (2019) CO5-10.

CO5-10 INAA and Ar-Ar Dating for Micro-sized Extraterrestrail Materials

R. Okazaki and S. Sekimoto[1]

Department of Earth and Planetary Sciences, Kyushu University

[1]*Institute for Integrated Radiation and Nuclear Science, Kyoto University*

INTRODUCTION: The major goal of this study is to determine the minor element compositions and Ar-Ar ages for submillimeter-sized extraterrestrial materials. We have been continually working to achieve this objective since 2013 (project #: 25066, PI: S.S.). In the Ar-Ar dating, concentrations of the parent (^{40}K) and daughter (^{40}Ar) nuclides are determined simultaneously. In order to obtain precise ages, it is important to adjust the irradiation condition, such as irradiation duration, neutron flux and neutron energy.

In the last year's proposal, we have investigated two irradiation conditions by using the hydraulic conveyor and the long-term irradiation plug. We have measured noble gases in JG-1 and orthoclase samples irradiated by the Hydro and Long-term irradiations. Based on the ^{39}Ar/^{40}Ar ratio determined for the Hydro and Long-term orthoclase samples, we found that the neutron flux parameter (J-value) for the Long-term irradiation is about half of that for the Hydro irradiation. Especially for NAA, it is important to evaluate the difference in the neutron energy spectrum between the two irradiation conditions. In this year's proposal, we conducted NAA for the standard minerals and a meteorite sample (Allende) that was already measured for NAA previously by using the Hydro irradiation.

EXPERIMENTS: Several hundred milligram samples were prepared from the Allende CV chondrite (Provided by Smithonian museum [1]) and our standard minerals (JB-1 [2], JP-1 [3], DTS-2b [4], orthoclase [5], sanidine, and wollastonite). Each of the samples was placed in a conical dimple (φ1, depth ~ 0.5 mm) of a sapphire disk (φ5.5, 1.5 mm thick), and covered with a sapphire disk (φ5.5, 0.3 mm thick). Each of the sapphire container was wrapped with pure aluminum foil. These Al-wrapped containers were stacked and sealed in the capsules for the Long-term irradiation. Condition of the Long-term irradiation as 122 hours under 1MW-operation + 18 h under 5MW-operation.

REUSLTS and DISCUSSION: After irradiation, the samples were moved to non-irradiated glass container with similar dimension from the sapphire one in order to reduce the radioactivity from the sapphire containers and Al foil. For the selected samples (Allende, JP-1, and DTS-2b), gamma ray measurements of radioactive nuclides were performed. The results are now analyzed to examine if the gamma ray spectrum of the Long-term irradiated Allende sample is essentially identical to the previous result of the Hydro irradiation. Based on the spectrum of the Long-term irradiated Allende sample, minor element concentrations in DTS-2b and JP-1 will also be calculated and compared with the compositions reported [3, 4].

After the gamma ray measurements, some of the irradiated samples were moved to Kyushu Univ. to measure noble gas isotopes. Noble gas analyses for these samples will be done this summer in order to evaluate the presence of interference isotopes produced by the low energy neutrons.

REFERENCES:

[1] E. Jarosewich *et al.*, Smithsonian Contributions to the Earth Sciences **27** (1987) 1-49.

[2] A. Ando *et al.*, Geochemical Journal **5** (1971) 151-164.

[3] https://gbank.gsj.jp/geostandards/igneous.html

[4] I. Raczek *et al.*, Geostandards Newsletter, **25** (2001) 77-86.

[5] S. Weiss, Mineralien Magasin Lapis. **16** (1991) 13–14.

CO5-11 Determination of Abundance of Rare Metal Elements in Seafloor Hydrothermal Ore Deposits by INAA Techniques-6: Evaluation of analytical accuracy

J. Ishibashi, T. Miyamoto, Y. Tada[1], Y. Sekiya[1], K. Yonezu[1], R. Okumura[2], Y. Iinuma[2] and K. Takamiya[2]

Department of Earth and Planetary Sciences, Faculty of Science, Kyushu University
[1]Department of Earth Resources Engineering, Faculty of Engineering, Kyushu University
[2]Institute for Integrated Radiation and Nuclear Science, Kyoto University

INTRODUCTION: Instrumental neutron activation analysis (INAA) has several advantages for geochemical tools to provide useful information for mineral exploration. For example, INAA enables highly sensitive multi-element analysis without geochemical pretreatment. We have conducted preliminary studies using mineralized samples collected from active seafloor hydrothermal fields, with a view to confirm and extend the range of application of this technique. Here, we report evaluation for analytical accuracy of INAA techniques.

EXPERIMENTS: We conducted a series of analysis of four materials (DS-1, CCU-1d, WMS-1a, and CH-4) from "Certified Reference Materials" which are provided by Natural Resource Canada in following three runs. In Run#1, samples were irradiated at Pn-3 (thermal neutron flux = 4.6×10^{12} n/cm^2/sec at 1 MW operation) for 0.5 minute, and the gamma ray activity was measured for 2-5 minutes after adequate cooling time (<5 hours). In Run#2, samples were irradiated at Pn-2 (thermal neutron flux = 5.5×10^{12} n/cm^2/sec at 1 MW operation) for 15 minutes, and the gamma ray activity was measured for 15 minutes after adequate cooling time (~25 hours). In Run#3, samples were irradiated at Pn-2 (thermal neutron flux = 5.5×10^{12} n/cm^2/sec at 1 MW operation) for 30 minutes, and the gamma ray activity was measured for 15 minutes after adequate cooling time (~30 hours).

RESULTS: Gamma ray intensities per 1Bq of As-76 or Mn-56 of each irradiated Certified Reference Material were calculated assuming that the elemental contents are identical to the reported values. Then, they were compared with gamma ray intensities of an artificial standard material (a piece of plastic filter loaded with known amount of As or Mn) which was irradiated in the same capsule. Their ratios (Reference/artificial standard) were plotted along the energy (keV) of the calculated gamma rays in Fig. 1.
The obtained ratios were basically within the range of 1.0 ± 0.1, which assures good analytical accuracies. However, some of them deviated from the ideal ratio. For example, CCU-1d (Cu-rich sulfide) and WMS-1a (Fe-rich sulfide includes 1% of Cu) showed rather poor accuracy (actually, the obtained ratios for WMS-1a were around 2.0 during Run#2). Since the deviation was more obvious in the gamma ray peaks in low energy, interference by Cu-66 would be responsible. Moreover, we have recognized that Cu-rich sulfides cause other samples in the same capsule to intensify activations of some nuclides in the case of long-time irradiation, as reported in the last year. It is important to minimize irradiation time for analysis of mineralized sulfides to obtain good accuracy.

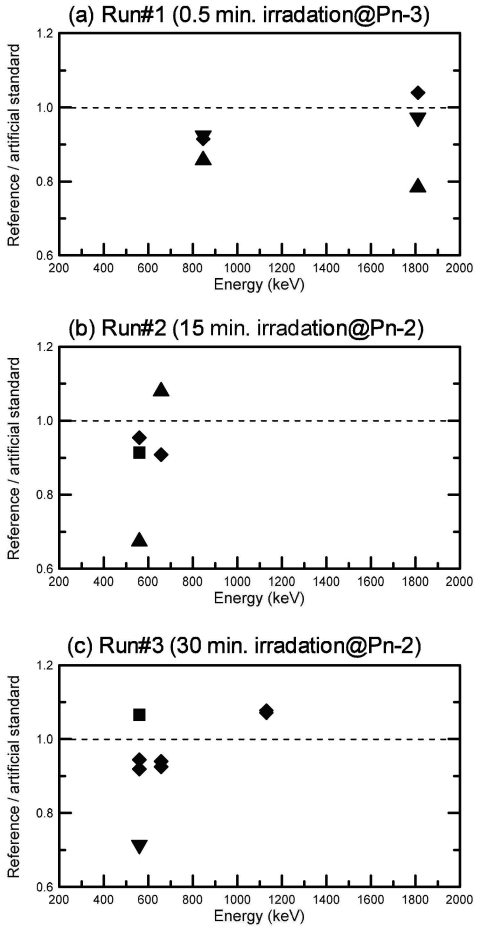

Fig. 1. Ratios of As-76 or Mn-56 gamma ray intensities of four materials (♦:DS-1, ▲:CCU-1d, ▼:WMS-1a, ■:CH-4) from the Certified Reference Materials to those of an artificial standard material irradiated in the same capsule.

CO5-12 Research on Earth Surface Processes by Use of Mineral Luminescence

N. Hasebe, M. Hamada[2], K. Miura[1], U. Uyangaa[1], R. Januar[1], Yudai Igarashi[1], K. Oohashi[2], Y. Minomo[2] and Y. Iinuma[3]

Institute of Nature and Environmental Technology, Kanazawa University

[1]Graduate School of Natural Science and Technology, Kanazawa University

[2]Graduate School of Science and Technology for Innovation, Yamaguchi University

[3] Institute for Integrated Radiation and Nuclear Science, Kyoto University

INTRODUCTION: Luminescence dating observes the natural accumulated radiation damage caused by radioisotopes such as U and Th as the form of glow after stimulation by heating or lightening. In this study, quartz vein distributed in Noto peninsula was collected and analysed by thermoluminescence (TL) and optical stimulated luminescence (OSL) methods. These quartz veins are found in the area where a small gold mine is located. There is a possibility that both of quartz vein and gold deposit is related and resulted from the thermal fluid circulation during the late stage of volcanic activity in the area.

EXPERIMENTS: A block of quartz vein with the size of ~15 cm in diameter was collected. This block was broken in the dark room and central small part was analysed. First, to examine the luminescence color, quartz was irradiated at gamma-ray irradiation facility at KUR to give a known dose of ~4 kGy. However, the luminescence emission was very dim and unable to identify the color. Remaining sample was measured by conventional OSL and TL methods. Annual dose is estimated from the U, Th, Sr, and K concentrations measured by LA-ICP-MS or X-ray fluorescence measurement (Ito et al., 2009, Stokes et al., 2003).

RESULTS: The OSL shows slowly decaying signal and suggests the small contribution of fast component. OSL signal is not very strong, and 14 measured aliquots show dispersed results (Fig. 1). Majority of samples showed equivalent dose less than 10 Gy. On the other hand, TL signal is strong. It is beyond the upper limit of artificial dose given by the in-house x-ray source, and could be estimated as around 3000 Gy (Fig. 2). Due to instrumental restrictions, it is not clear this value is close to the saturation or not. Therefore, this estimate could be the minimum value. The big difference between OSL and TL data may reflect the sample storage condition. Because quartz is transparent mineral, the inner samples may also be affected by the light and have lost the signal for OSL Based on the TL results and annual dose, the estimated ages is older than 4.2 Ma. Considering that main volcanic activity was in the Miocene related to Japan Sea opening, this quartz vain might be formed during or just after the main volcanic activity.

REFERENCES:

Ito, K., Hasebe, N., Sumita, R., Arai, S., Yamamoto, M., Kashiwaya, K., Ganzawa, Y., 2009. LA-ICP-MS analysis of pressed powder pellets to luminescence geochronology. Chemical Geology 262, 131-137.

Stokes, S., Ingram, S., Aitken, M.J., Sirocko, F., Anderson, R., Leuschner, D., 2003. Alternative chronologies for Late Quaternary (Last Interglacial-Holocene) deep sea sediments via optical dating of silt-sized quartz. Quaternary Science Rev. 22, 925-941.

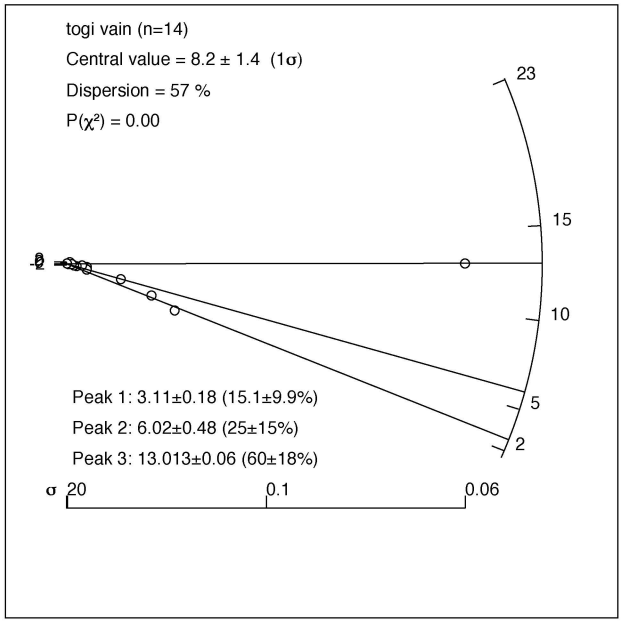

Fig. 1. Radial plot of fourteen OSL data (Gy).

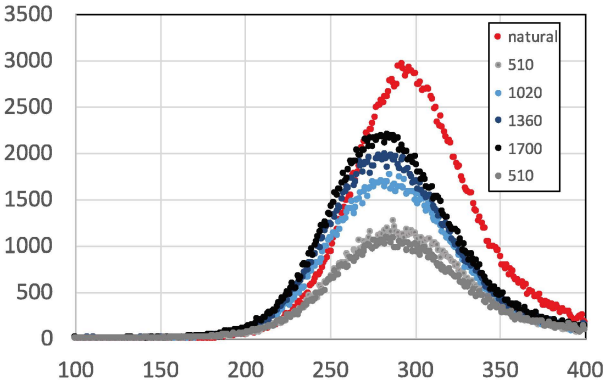

Fig. 2. Example of TL profile. Numerical numbers in the legend represent a given dose (Gy).

CO5-13 Geochemistry of unbrecciated eucrite, Northwest Africa 10962

N. Shirai, S. Sekimoto[1], M. Ebihara[2]

Department of Chemistry, Tokyo Metropolitan University

[1]*Institute for Integrated Radiation and Nuclear Science, Kyoto University*

[2]*Department of Earth Sciences, Waseda University*

INTRODUCTION: Howardite, eucrite and diogenite (HED meteorites) are the largest group of achondrite which are thought to have been derived from asteroid Vesta. Recently, the Dawn mission confirmed that the Vesta's surface is mineralogically and chemically similar to HED meteorites [1]. Depletions of siderophile elements in HED meteorites suggest that HED meteorites are products of differentiation [2]. Therefore, HED meteorites are important to elucidate the core formation of Vesta. Eucrites are mostly composed of pyroxene and plagioclase. As almost all eucrites are brecciated, it is difficult to bring out their primitive chemical compositions. Some eucrites (e.g., ALH 76005) were reported to contain foreign meteoritic components [e.g., 3]. From these materials, siderophile elements abundances for eucrites may have been modified. A few unbrecciated eucrites also have been found. As siderophile elements abundances for these unbrecciated eucrites were not affected by the incorporation of foreign materials, its chemical compositions give us the important information about the differentiation processes of Vesta. We determined elemental abundances for Northwest Africa (NWA) 10962, which was classified into unbrecciated eucrites [4] by using INAA and aimed to chemically characterize this meteorite in comparison with those for other eucrites.

EXPERIMENTS: A chip of NWA 10962 weighing 1.4 g was carefully ground in an agate mortars in order to obtain the representative chemical composition. This powder sample was firstly irradiated for 10 s at the pn-3 of the Institute for Integrated Radiation and Nuclear Science, Kyoto University with thermal and fast neutron fluxes of 4.6 x 10^{12} and 9.6 x 10^{11} $cm^{-2}s^{-1}$, respectively. After irradiation, sample was immediately measured for gamma-ray emissions. After 24 hours, the same sample was irradiated fro 3 h at the pn-2 of the Institute for Integrated Radiation and Nuclear Science, Kyoto University, with thermal and fast neutron fluxes of 5.6 x 10^{12} and 1.2 x 10^{12} $cm^{-2}s^{-1}$, respectively. The sample was measured three times for gamma-rays after different cooling intervals over a one-month period. JB-1 and the Smithsonian Institution Allende meteorite sample were used as the standard reference material.

RESULTS AND DISCUSSIONS: Twenty elements could be determined by using INAA. Major elements abundances of NWA 10962 are similar to those of the common Main-group eucrites. However, it is noticed that trace element abundances of NWA 10962 are slightly different from those of the common Main-group eucrites. La abundances are plotted against Hf abundances for eucrites in Fig. 1. On this plot, eucrites are classified into the three subgroups; cumulate eucrites, basaltic eucrites and residual eucrites [5]. As clearly confirmed in Fig. 1, NWA 10962 belongs to residual eucrites. In terms of rare earth elements (REEs) abundances, NWA 10962 is different from the common eucrites. NWA 10962 is slightly depleted in light REEs. Its REE pattern exhibits a pronounced positive Eu anomaly, which bears some resemblance to cumulate eucrites and residual eucrites. Thus, NWA 10962 is classified as residual eucrites.

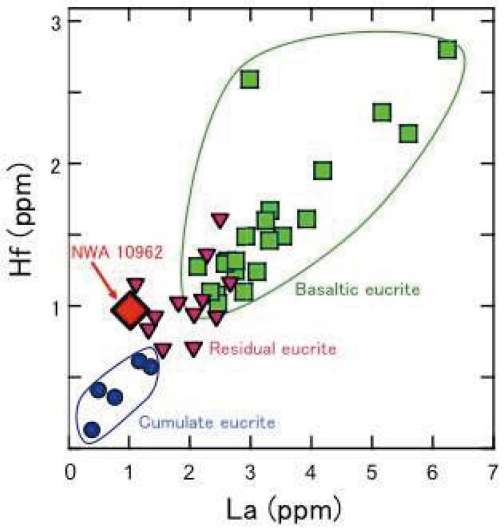

Fig. 1. La vs. Hf for euceites.

Based on petrology [4], it was reported that NWA 10962 contain about 1% of FeNi metal. It is examined whether this FeNi metal endogenously produced or not based on its elemental abundances. To extract FeNi metal, the irradiated sample was leached with 6M HCl in an ultrasonic bath for 10 min. The obtained solution was measured by gamma-ray emissions. For this solution, Fe and Co could be determined, while Ir and Ni could not be detected. Nickel/Co and Ir/Co ratios of NWA 10962 are different from those of iron meteorites and FeNi metal for chondrites. These elemental ratios of NWA 10962 are lower than those of FeNi metal of Camel Donga, which was considered to be produced by reduction of FeO and FeS [6]. Thus, FeNi metal of NWA 10962 is not foreign meteoritic components and it is concluded that NWA 10962 is suitable for discussing about differentiation of asteroid Vesta.

REFERENCES:

[1] M. C. De Sanctis *et al.*, Science, **336** (2012) 697-700.
[2] K. Righter and M. J. Drake, Meteorit. Planet. Sci., **32** (1997) 929-944.
[3] N. Shirai *et al.*, Earth Planet. Sci. Lett., **437** (2016) 57-65.
[4] A. Bouvier *et al.*, Meteorit. Planet. Sci., **52** (2017) 2411.
[5] A. Yamaguchi *et al.*, Geochim. Cosmochim. Acta, **73** (2009) 7162-7182.
[6] H. Palme *et al.*, Meteoritics, **23**, 49-57 (1988).

CO5-14 Neutron Activation Analysis of Environmental Samples

Y. Oura and Md. S. Reza

Graduate School of Science, Tokyo Metropolitan University

INTRODUCTION: Environmental pollution is an important issue for our healthy life. Determination of elemental composition is one of the ways for an environmental examination. For example, shellfish are commonly used for an assessment of ocean environment. In this case soft tissues in shellfish (e.g. mussels) are mainly analyzed for elemental concentration, whereas, shells seem not to be analyzed. Thus, we tried to determine elemental concentrations in shell if they are effective in assessing the coastal/lake environment. In this work, Japanese basket clam (scientific name: corbicula japonica) living in brackish-water lake was selected because it is easily available, and it has an easily handled size. For atmospheric environment, attention has been focused on the effects of very small particles called PM2.5 on human health in recent year. Elemental composition of particulates plays an important role for estimation of their origins. We have collected PM2.5 particulates at Hachioji, Tokyo and determination of elemental concentration in PM2.5 particulate was continued from last year.

EXPERIMENTS:

Shells

Japanese basket clam (Yamato Shijimi) yielded at Jyusan Lake in Aomori prefecture were got from a supermarket. After discarding soft tissues, clamshells were cleaned properly by ultrapure water using an ultrasonic water bath. Then they were made powder after drying. Ten different parts of clamshell (one clam contains two parts) from 5 individuals were subjected to analysis. About 180 mg of each sample was irradiated together with reference materials (GSJ JCp-1, JCt-1, and JB-1a) for 30 seconds and 4 hours at KUR (1 MW operation). After irradiation gamma-rays were measured by HPGe detector.

PM2.5

PM2.5 particulates have been collected on a Nucleopore polycarbonate filter of 0.2 μm of pore size for three weekdays every week at a rooftop of a building in Minami-Osawa campus of Tokyo Metropolitan University. Polycarbonate filters on which PM2.5 was collected were cut in half, then one half was subjected to analysis. Filter sample in clean polyethylene bag was irradiated together with reference materials (NIST 1648, NIST 1632c, NIES No.8, and GSJ JB-1a) for 5 minutes at KUR (1 MW operation) and 1 hour at KUR (5 MW operation). After irradiation, gamma-rays were measured by Ge detector.

RESULTS:

Shells

Thirteen elements (Na, Cl, Ca, Sc, Cr, Mn, Fe, Co, Zn, Br, Sr, Zr, and Ba) were detected under the analytical conditions in this study. The main element was Ca, whose concentrations (ca. 38 %) were almost same as those in JCp-1 (coral) and JCt-1(giant clam). Sodium concentrations (ca. 4100 mg/kg), which were the second highest concentration among determined elements in this work, were also similar to those in JCp-1 and JCt-1.

Elemental concentrations of two parts of clamshell of an individual were consistent within their uncertainties for most elements with exception of Cr and Fe. Iron concentrations of one pair and Cr concentrations of three pairs of five pairs were inconsistent.

Fluctuations of concentrations among five individuals were small for most elements. Relative standard deviations were smaller than 7 % for Ca, Na, and Sr, which are the three main elements in this work. For Mn, Cr, and Fe, one individual has high Mn concentration (about 4 times higher than others) and another individual has extremely high Fe and Cr concentrations (about 15 times and 5 times higher, respectively). Ca, Sr, and Ba belong to alkaline-earth metals. Concentration ratios of Sr/Ca were relatively consistent among five individuals, whereas, Ba/Ca and Ba/Sr were varied. Their maximum ratio values were about two times higher than minimum ratio values.

PM2.5

Mass concentrations of PM2.5 particulates collected in 2019 ranged from 3 to 36 μg m^{-3}, and their median of 11 μg m^{-3} was the same as the median in 2018, when the collection period was different from one in 2019. Determined elemental concentrations in PM2.5 particulates collected in 2019 are compared to those in 2018 in Fig.1. The median values of elemental concentrations in 2018 and 2019 are similar in general like the mass concentrations. Atmospheric environment around our university seems not to be different yearly between in 2018 and 2019 on the average.

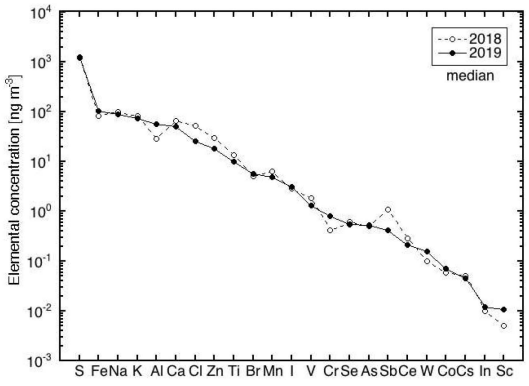

Fig.1. Median values of elemental concentrations in PM 2.5 collected in 2018 and 2019. Elements are arranged in order of increase of their median in 2019.

CO5-15 Bulk Chemical Compositions of CB and CH Chondrites

M. Ebihara, Y. Hidaka, T. Fujimura, M. Kamata, S. Koshimizu, N. Shirai[1] and S. Sekimoto[2]

Department of Earth Science, Waseda University
[1]Department of Chemistry, Tokyo Metropolitan Univ.
[2]KURNS, Kyoto University

INTRODUCTION: CB and CH chondrites are metal rich chondrite groups [1, 2] and their oxygen isotopic compositions show a close relationship to CR chondrites [3]. Recently, the petrogenesis of CB chondrites came to be considered as the condensation from impact-induced vapor plume [4, 5]. According to the similarity of oxygen isotopic composition between CB and CH chondrites, the parent bodies of these chondrites might exist close to each other. Then, how impact processes affected the origin and the evolution of CH chondrites? What was the difference between CB and CH chondrites? These questions are quite interesting. Impact-induced vaporization causes volatility loss of elements, so chemical compositions and isotopic compositions must become powerful tool to discuss these issues.

Bulk chemical compositions of CB and CH chondrites have been scarcely reported and have been poorly discussed. Here, we report the preliminary results of our bulk chemical analyses for CB and CH chondrites, MacAlpine Hills (MAC) 02675 (CB_b), Asuka 881020 (CH), Asuka 881541 (CH), Patuxent Range (PAT) 91546 (CH) and Pecora Escarpment (PCA) 91467 (CH).

EXPERIMENTS: Bulk chemical compositions of 1 CB_b chondrite (MAC 02675) and 4 CH chondrites (Asuka 881020, Asuka 881541, PAT 91546 and PCA 91467) have been determined by INAA and ICP-MS in this study. A chip sample weighing 130-440 mg of each meteorite was crushed into small chips and fine grains. Small fractions weighing ~40 mg of each meteorite were used for INAA.

RESULTS: The Mg-, CI-normalized and Ni-, CI-normalized chemical compositions of CB_b and CH chondrites obtained by INAA are shown in Fig. 1. The elements are sorted in decreasing of volatility [6]. In Fig. 1a, refractory lithophile element (Al, Ca, and Sc) abundances in CB_b chondrite (CI x ~1.5) are significantly higher than those of CH chondrites (CI x ~1). The Cr/Mg and Mn/Mg ratios in CB_b chondrite (2.6 and 0.28 x CI) are clearly higher and lower than those of CH chondrites (1.1 and 0.45 x CI). The range of Na/Mg ratios are nearly identical between CB_b (0.20-0.32 x CI) and CH (0.18-0.34 x CI) chondrites.

In Fig. 1b, refractory siderophile element (Os, Ir, Ni, Co) abundance patterns are identical between CB_b and CH chondrites, but as volatility increases, CB_b and CH chondrites show different chemical compositional characteristics. The principal differences are shown in Mn and Cr abundances. The Mn/Ni and Cr/Ni ratios are significantly lower in CB_b chondrite (0.022 and 0.21 x CI, respectively) than those of CH chondrites (0.23 and 0.56 x CI).

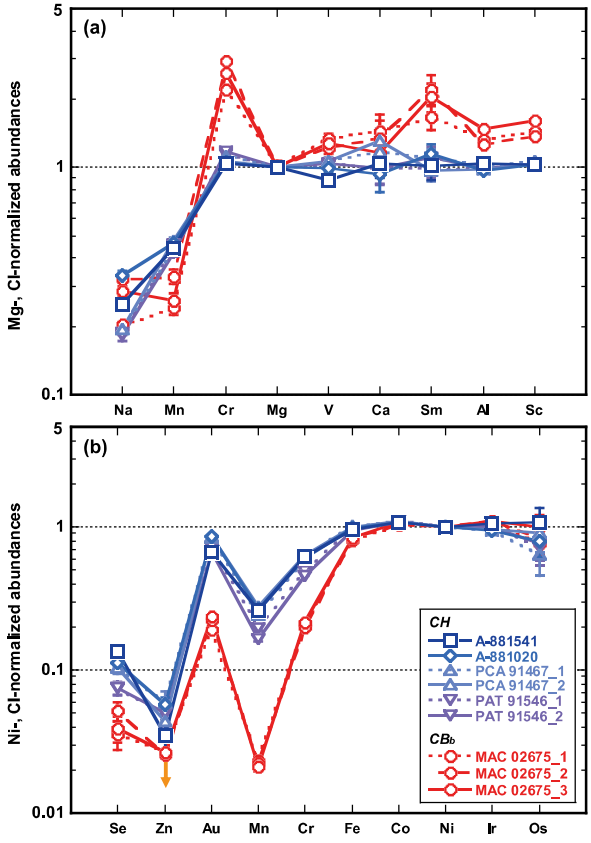

Fig. 1. Bulk chemical compositions of CB_b and CH chondrites obtained by INAA. Fig. 1a shows Mg- and CI-normalized lithophile element abundance patterns. Fig. 1b shows Ni- and CI-normalized siderophile and chalcophile element abundance patterns. CI chondrite data used for normalization are from [7].

REFERENCES:

[1] A. Bischoff *et al.* Geochim. Cosmochim. Acta, **57** (1993) 2631-2648.
[2] M. K. Weisberg *et al.* Meteoritics & Planet. Sci., **36** (2001) 401-418.
[3] A. N. Krot, Meteoritics & Planet. Sci., **37** (2002) 1451-1490.
[4] A. V. Fedkin *et al.* Geochim. Cosmochim. Acta, **164** (2015) 236-261.
[5] M. Weyrauch *et al.* Geochim. Cosmochim. Acta, **246** (2019) 123-137.
[6] B. Fegley, in *The Chemistry of Life's Origins,* edited by J. M. Greenberg et al. (Kluwer, Dordrecht, 1993) 75-147.
[7] E. Anders and N. Grevesse, Geochim. Cosmochim. Acta, **53** (1989) 197-214.

CO5-16 Determination of Cl, Br and I contents in geochemical reference samples by radiochemical neutron activation analysis - revisited

M. Ebihara, S. Sekimoto[1] and N. Shirai[2]

Department of Earth Science, Waseda University
[1]KURNS, Kyoto University
[2]Department of Chemistry, Tokyo Metropolitan Univ.

INTRODUCTION: We have been determining three halogen contents in geochemical and cosmochemical samples by using radiochemical neutron activation analysis (RNAA). (Here, halogens denote chlorine, bromine and iodine). To verify the reliability of analytical data for rock samples, geochemical reference samples are to be routinely analyzed together with unknown samples. For such a verification, it is essential that reliable data are available for some (at least one) reference sample for target elements (here, halogens). Because it was not the case for halogens, we have been repeatedly analyzed several geochemical reference samples to contribute for making the situation better and establish reliable data base for halogens in selected geochemical reference samples. To continue to approach to our goal, we have analyzed five geochemical reference samples prepared by Geological Survey of Japan (JR-3) and United States Geological Survey (SBC-1, DTS-2a, AGV-2 and GSP-2) and encountered an unexpected problem in evaluating our halogen data., which is described in this report

EXPERIMENTS: About 100-200 mg of each powder samples was weighed, inserted into a clean, small plastic vial, which was then sealed in a clean polyethylene bag. For quantification of halogens, chemical standard solutions of halogens were prepared by dissolving appropriate amounts of potassium halides (KCl, KBr and KI) in pure water. In addition, a KOH solution was prepared to adjust the alkalinity in iodine solutions. An appropriate amount of each halogen solution was dropped onto a paper disk (17 mm ϕ), weighed, dried under a heat lamp and doubly sealed into polyethylene bags. An extreme care was taken when preparing the iodine reference sample, for which two set of samples (one with KOH and another without KOH) were prepared. Two geochemical reference samples, together with a set of three (or four) reference samples, were irradiated for 10 min with a thermal neutron flux of 3.3 x 10^{12}cm^{-2} s-1 at Kyoto University Research Reactor of KURNS.

RESULTS: The Analytical results of the three halogens for the five geochemical reference samples are summarized in Table 1. The data obtained in this experiment are compared with our previous data published [1, 2]. For AGV-2 and GSP-2, additional literature values [3] also are shown. Our Cl data are consistent with our old data, being within 10%. The literature data of [3] are somewhat higher than ours but the difference may be permissible. The degree of agreement between our data (old and new) and among the three sets seems to become worse for Br and much worse for I. For Br, a systematic difference can be seen between our present data and previous data; the present data are 40% to 8% lower than the old data. In contrast, the literature data of [3] are 3 to 5 times higher than those of our literature values [1, 2]. For I, the large/small relation is different from that for Br; our present data are 19% to 87% smaller than the previous values, but larger than the literature values of [3]. Between our present data and our old data of [2] or [3], much smaller disagreement can be noticed for [2] than for [3], although statistics are poor. At this stage, a conclusive explanation for the disagreement of Br and I data between our present and past experiments. has not been attained yet. However, considering any conceivable possibility, we have just come up with a reasonable explanation. Once the reactor becomes usable, we will conduct the experiment to identify the source for yielding unsystematic as well as systematic inconsistencies.

REFERENCES:

[1] S. Sekimoto and M. Ebihara, Geostand, Geoanal. Res., **41** (2017) 213-219.
[2] S. Sekimoto and M. Ebihara, Anal. Chem., **85** (2013) 6336-6341.
[3] T. He, Z. Hu, W. Zhang, H. Chen, Y. Liu, Z. Wang and S. Hu, Anal. Chem., **91** (2019) 8109-8114.

Table 1. Analytical results (in μg/g) of halogens in geochemical reference samples*

	Cl	Br	I
SBC-1	22.5 (24.9)	0.325 (0.355)	0.670 (5.07)
DTS-2b	10.5 (10.7)	0.098 (0.093)	0.119 (0.789)
AGV-2	75.9 (72.8; 84.0)	0.075 (0.101; 0.27)	0.034 (0.197; 0.013)
GSP-2	349 (363; 389)	0.068 (0.117; 0.57)	<DL (0.075; 0.013)
JR-3	126 (134)	0.450 (0.577)	0.390 (0.482)

* Our present data are followed by previous values [2] (and literature values [3] for AGV-2 and GDP-2) in parentheses.

CO5-17 Spatial Distribution of Halogen Compositions in the Wedge Mantle-derived Metaserpentinite Body in Southwest Japan

H. Sumino, J. Ren, A. Takenouchi, M. Koike, R. Okumura[1], Y. IInuma[1], H. Yoshinaga[1] and S. Sekimoto[1]

University of Tokyo
[1] Institute for Integrated Radiation and Nuclear Science, Kyoto University

INTRODUCTION: Mantle wedge - the triangular shaped piece of mantle that lies above subducted plate (slab) and below the overriding plate - is essential for transporting water into mantle at subduction zone. The oceanic plate is hydrated before subducting, and then dehydrates at subduction zone to supply water to the mantle wedge. However, the details of hydration and dehydration processes remain debated. A major question is the exact depth where water is released, because water would notably change the chemical and physical properties of rocks and play an important role in volcanism and seismicity at subduction zones.
The heavy halogens (Cl, Br, I) are highly soluble in fluids, and hard to enter minerals during partial melting of peridotite (the major type of rock in the mantle) [1]. Furthermore, their ratios, especially I/Cl ratios vary up to several orders of magnitude among different reservoirs in subduction zones (e.g. mantle, subducting slab, sediments, and sedimentary pore fluids – water trapped in pore space in sediments), making them good tracers for fluid sources in subduction systems [2,3].
In this study, we analyzed the halogens in rock samples of an ancient slab-wedge mantle boundary [4] and observed the spatial distribution of halogen compositions, in order to constrain how the fluids from subducted plate modified the mantle wedge and how volatiles moved in subduction zones.

SAMPLES AND BACKGROUND: The Sanbagawa belt, which lies on the south of Median Tectonic Line, is composed of various kinds of metamorphic rocks which experienced subduction to deep in the Earth. It is proposed that Shiraga metaserpentinites (hydrated and deformed peridotites) in the Sanbagawa belt are originated from wedge mantle. Further, a previous study shows that the eastern boundary of Shiraga metaserpentinite preserved primary information about the ancient slab-wedge mantle interface [4]. In contrast, various types of schists represent altered slab materials that surrounding serpentinite body.

EXPERIMENTS: Samples were neutron irradiated in KUR to convert halogens (^{37}Cl, ^{79}Br, ^{127}I) to noble gas proxies (^{38}Ar, ^{80}Kr, ^{128}Xe). The extraction (crushing and heating) and measurement of these noble gas proxies were analyzed with a mass spectrometer at the University of Tokyo [5]. The crushing method releases halogen-derive noble gases from fluid inclusions, which are thought to partially preserve the information of the original fluid that reacted with rocks. While the data obtained with heating of residual powder after crushing mainly represents the composition of halogens in solid phase, i.e. crystal lattice of minerals.

RESULTS: The halogen data of crush extraction show markedly higher I/Cl ($1.5 \times 10^{-4} – 3 \times 10^{-3}$) comparing with normal upper mantle (4×10^{-5}), seawater ($\sim 10^{-6}$), oceanic crust ($\sim 10^{-6} – 10^{-7}$), or other reservoirs in subduction system. This is similar to the mantle wedge peridotites that come from ~100 km depth [2], which are considered to originate from sedimentary pore fluids at seafloor.
It is notable that “Si-rich serpentinite”, samples near the slab wedge mantle boundary have evidently higher I/Cl than others. Within the serpentinite body, I/Cl tend to decrease with the distance from the boundary, which means that the original fluid with high I/Cl may come through/from the slab wedge mantle interface, then diffused upward into the mantle wedge and was gradually diluted by normal mantle with low I/Cl. In addition, this trend is not continuous at the slab wedge mantle boundary, implying the original fluid not necessarily came directly from the adjacent slab materials.

CONCLUSIONS: The halogens composition of Shiraga serpentinite body shows similar elemental ratios with that from deeper mantle wedge peridotites, which are considered to originate from the same source as sedimentary pore fluids. Based on the spatial distribution of I/Cl, the original fluid could come through slab wedge mantle interface, and then transfer upward into the mantle wedge.

REFERENCES:
[1] D. M. Pyle & T. A. Mather. Chem. Geol., **263** (2009) 110-121.
[2] H. Sumino *et al.*, Earth Planet. Sci. Lett., **294** (2010) 163-172.
[3] M. A. Kendrick *et al.*, Earth Planet. Sci. Lett., **365** (2013) 86-96.
[4] H. Kawahara *et al.*, Lithos, **254-255** (2016) 53-66.
[5] N. Ebisawa *et al.*, J. Mass Spectrom. Soc. Jpn., **52** (2004) 219-229.

CO5-18 Fission track age and thermal history of clay deposit of the Tsuchihashi Mine

H. Ohira and Y. Sampei

Department of Earth Science, Shimane University

INTRODUCTION: Fission track (FT) dating was carried out to estimate ages of hydrothermal alteration to form clay deposit of the Mitsuishi mining area at Bizen City, Okayama prefecture. Several clay deposits are located near the ring fault of eastern margin of the Wake Caldera, implying that hydrothermal fluid circulation along the ring fault contributed to form the deposit of this area [1]. The Tsuchihashi mine is typical mine operating underground quarry, yields high grade clayey rocks used for raw materials of refractories and ceramics. Several zones (such as pyrophyllite, sericite and silica rock) develop in response to conditions of hydrothermal alteration [2]. Samples were collected from above zones and U-Pb dating was also applied to estimate eruption age of host pyroclastic rocks.

EXPERIMENTS: Sample was crashed, sieved and heavy minerals were concentrated using conventional method of heavy liquid and magnetic separator. Minerals were mounted in PFA Teflon, and polished to reveal a complete internal surface, and etched in NaOH-KOH eutectic melt at 225˚C [3] for 12-15 hours. Samples were irradiated at pneumatic tube of graphite facility (Tc-pn) of Kyoto University Reactor (KUR). After irradiation, external detectors (mica) were etched in 46% HF at 25˚C for 6-7 minutes (for mineral mounts) and for 20-50min (for NIST-SRM612 glass). FT density was measured at 1000× magnification with a dry objective. U-Pb dating was carried out in cooperation with Dr. Hisatoshi ITO of Central Research Institute of Electric Power Industry (CRIEPI). Dating was performed using a Thermo Fisher Scientific ELEMENT XR magnetic sector-field ICP-MS coupled to a New Wave Research UP-213 Nd-YAG laser at CRIEPI [4].

RESULTS: FT ages obtained are 72.4±2.5Ma and 72.6±2.6Ma (silica rock zone), 75.9±2.7Ma (pyrophyllite zone) and 77.9±3.4Ma (sericite zone). These FT ages are relatively compatible with previously reported K-Ar ages for clay veins (78.1Ma, 74.0Ma, 73.0Ma) and clayey rocks (80.0Ma, 78.8Ma, 77.8Ma) [5]. Newly obtained U-Pb ages are 78.0 ± 1.5Ma (silica rock zone) and 77.3±1.8Ma (sericite zone). These ages are slightly younger than previously reported age (82.4±0.6M [2]). Ages versus closure temperature plot are shown in Fig. 1. U-Pb ages probably correspond to stage of eruption of host pyroclastic rocks or magmatic activity causing caldera structure, considering with its high closure temperature (800 ℃ < [6]). The variation of U-Pb ages (77-82Ma) should be examined in more detail. Previously reported K-Ar age (73-80Ma, [5]) probably correspond to a period of culmination of hydrothermal activity which formed several clay zones after caldera formation. Considering relatively lower closure temperature of FT methods (230℃<), FT ages (73-78Ma) probably indicate a period when sample cooled below 240℃ during attenuation of hydrothermal alteration. The youngest FT age from silica rock zone (72.4-72.6Ma) show a period of latest stage of hydrothermal activity, which was probably sustained for a certain period (several Ma) after eruption of host pyroclastic rocks or caldera formation.

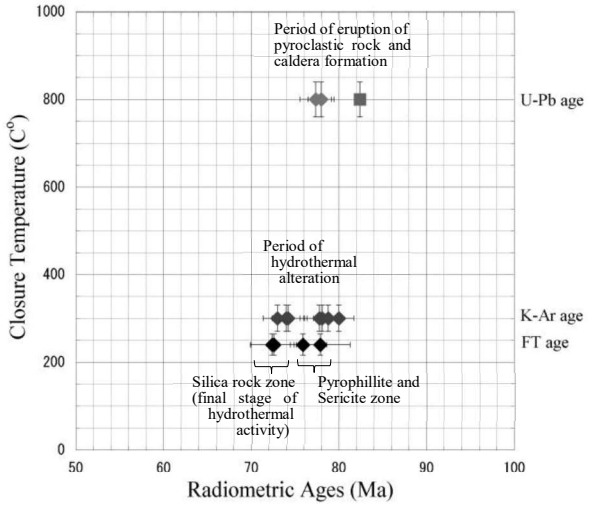

Fig.1 Closure temperature vs. Age plot.

[1] ISHIHARA S. and IMAOKA T., 1999, Resource Geology, 49, 157-162.
[2] Sato D., Yamamoto T. and Takagi T., 2016, Geology of the Banshu-Ako district. Quadrangle Series, 1:50000, Geological Survey of Japan, AIST, 68p (in Japanese with English abstract).
[3] Gleadow A.J.W. *et al.*, 1976, Earth and Planetary Science Letter, 33, 273-276.
[4] Ito H. *et al.,* 2017, Quaternary Geochronology 40, 12-22.
[5] Hongu H., Kitagawa R. and Nishido H., 2000, Clay Science (Nendo Kagaku) 40, 46-53.
[6] Cherniak, D.J. and Watson, E.B., 2000, Chemical. Geology, 172, 5.

CO5-19 ^{40}Ar-^{39}Ar Dating of Extraterrestrial Materials in KURNS

N. Iwata, S. Sekimoto[1], R. Okazaki[2] and Y. N. Miura[3]

Faculty of Science, Yamagata University
[1]Institute for Integrated Radiation and Nuclear Science, Kyoto University
[2]Department of Earth and Planetary Sciences, Kyushu University
[3]Earthquake Research Institute, University of Tokyo

INTRODUCTION: Radiometric dating is useful tool for unveiling formation and evolution process of planetary material. ^{40}Ar-^{39}Ar method is invaluable to date the timing of heating events on planetesimal and asteroid (e.g. Swindle et al. (2014) [1]). Especially, ^{40}Ar-^{39}Ar dating method with laser heating technique is suitable for small amount sample (e.g. Kelley, 1995 [2] and Hyodo, 2008 [3]).

For example, tiny material returned from asteroid 25143 Itokawa is dated using laser heating ^{40}Ar-^{39}Ar dating method by Park et al. (2015) [4] and Jourdan et al. (2017) [5]. Park et al. (2015) reported an age of 1.3 ± 0.3 Ga. Jourdan et al. (2017) reported an age of 2.3 ± 0.1 Ga. These ages indicate the timing of catastrophic events which were occurred on Itokawa's precursor body. Combining the ^{40}Ar-^{39}Ar ages and other chronological data, Terada et al. (2018) [6] overviewed the time evolution of the Itokawa asteroid. Similar investigation, the integration of multichronological data is proposed to the material that recovered from asteroid 162173 Ryugu and other extraterrestrial materials. ^{40}Ar-^{39}Ar dating will play an important role within the investigations.

To implement of dating of extraterrestrial material by ^{40}Ar-^{39}Ar method, we will develop a system which includes gas extraction and gas purification line in KURNS (Fig. 1). A continuous Nd-YAG laser (~60 W) extract gas from neutron irradiated sample. The extracted gas is purified and encapsulated into metal gas trap. The purified gas in the metal gas trap is transported to laboratories of noble gas analysis (e.g. Kyushu University) and argon isotope of the gas is analyzed using noble gas mass spectrometer. Further, we have a plan to connect a quadrupole mass spectrometer to this system in the future, in order to perform on-lined laser heating ^{40}Ar-^{39}Ar dating.

EXPERIMENTS: Dr. R. Okazaki of Kyushu University designed the system. The gas extraction part consists of a sample chamber. The gas purification part consists of a Sorb-AC getter pump. Ti-Zr getter will be added as needed. Connecting port is used for jointing gas purification part and gas trap tree and/or the quadrupole mass spectrometer as needed. Whole of the parts are evacuated by two oil rotary pumps and two turbo molecular pumps to ultra-high vacuum condition.

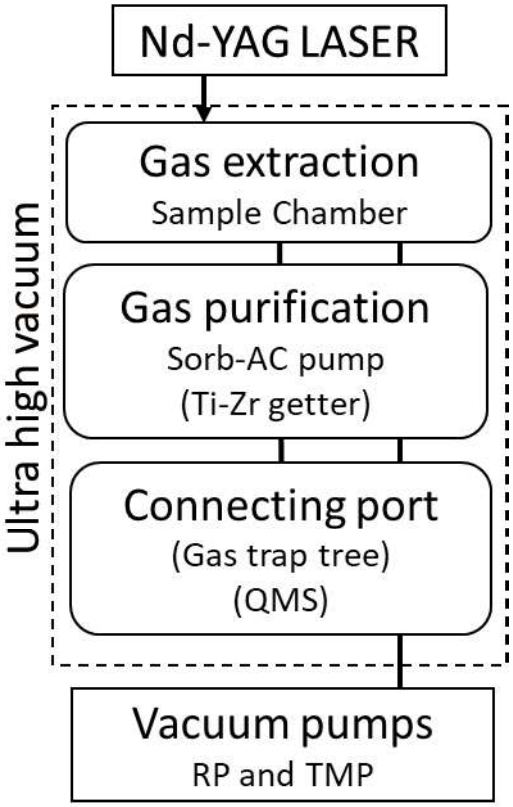

Fig. 1. Outline of gas extraction and purification line in KURNS. Components in parentheses are optional.

RESULTS: We started assembling of the laser-heating gas extraction and purification system in KURNS in 2019. The design work and configuration of the system is almost completed. Unfortunately, the constructing work was interrupted by influence of epidemic prevention of COVID-19. We are going to continue setting the system up during 2020.

REFERENCES:

[1] T. D. Swindle *et al.*, in *Advances in ^{40}Ar/^{39}Ar Dating: from Archaeology to Planetary Sciences*, edited by Jourdan, Mark, Verati (Geol. Soc., London, Spec. Pub. **378**, 2014) 333-347.
[2] S. P. Kelley, in *Microprobe techniques in the earth sciences*, edited by Potts, Bowles, Reed, Cave (Chapman & Hall, London, 1995) 327-358.
[3] H. Hyodo., Gondwana Res. **14** (2008) 609-616.
[4] J. Park *et al.*, Meteorit. and Planet. Sci., **50** (2015) 2087-2098.
[5] F. Jourdan *et al.*, Geology, **45** (2017) 819-822.
[6] K. Terada *et al.*, Sci. Rep., **8** (2018) #11806.

CO5-20 Neutron activation analysis of carbonate reference materials: coral (JCp-1) and giant clam (JCt-1)

S. Sekimoto, Y. Homura[a], V.D. Ho[1], M. Inagaki, N. Shirai[2], T. Ohtsuki

Institute for Integrated Radiation and Nuclear Science, Kyoto University
[1]Nuclear Research Institute, Vietnam Atomic Energy Institute
[2]Department of Chemistry, Tokyo Metropolitan University
[a]Present address: Novaltis Farma

INTRODUCTION: Geochemists are often interested in the abundance of halogen elements in geochemical materials such as crustal rocks, mantle materials, and meteorite samples, because halogens play an important role in investigating the petrogenesis of such materials and assist in tracing their origins and/or precursor materials [1-3]. In our previous work, radiochemical neutron activation analysis (RNAA) was refined to accurately determine even trace amounts of halogens (chlorine, bromine, and iodine) in sedimentary rock reference samples [4]. Subsequently, U.S. Geological Survey (USGS) geochemical reference materials were subjected to RNAA, and the data obtained were compared with literature data [5]. The two kinds of carbonate reference materials investigated here, JCp-1 (Coral) and JCt-1(Giant Clam), are prepared by the Geological Survey of Japan/National Institute of Advanced Industrial Science and Technology (GSJ/AIST), and the concentrations of many major and a few trace elements in these materials have been determined [6-8]. Data about the halogen contents in these materials is expected to significantly contribute to a better understanding of the chemistry of seawater and the marine environment, since halogens (especially iodine) are known to be extremely useful in investigating the geochemical circulation of terrestrial materials [9]. However, to our knowledge, there is not much data on the halogen contents of these carbonate materials.

The present study aims to use RNAA and instrumental NAA (INAA) to determine trace amounts of three halogens in JCp-1 and JCt-1, together with other elements. Based on the halogen data, the differences between the two carbonate reference materials is investigated. The INAA values obtained in the present study are compared with literature values, and the consistency between our data and the data from known literature is evaluated.

EXPERIMENTS: The procedure of RNAA used in this work has been reported previously.[4] For INAA studies, about 50 mg of JCp-1 and JCt-1, together with a similar amount of two kinds of USGS basalt reference materials for quantification, BCR-2 and BHVO-2, was irradiated for 4 h using KUR to measure the relatively long-lived nuclides (with half-lives > 24 h; ^{46}Sc, ^{59}Fe, ^{60}Co, ^{85}Sr, ^{134}Cs, ^{140}La, ^{141}Ce, ^{152}Eu, ^{181}Hf, and ^{182}Ta, and ^{239}Np) produced by the (n,γ) reaction in each material. As for ^{239}Np, the (n,γ) reaction is followed by γ-decay. Additionally, the nuclides ^{24}Na, ^{28}Al, and ^{49}Ca in these materials were also measured by irradiating the samples for 10 s. Since the Mn content in the two carbonate materials of interest in this study (JCp-1 and JCt-1) is known to be very low relative to that in geochemical materials, irradiation for 20 min was required for the measurement of ^{56}Mn. For determination of the Mn content, a chemical standard solution of Mn was utilized. An appropriate amount of Mn solution (100 mg kg^{-1}, typically) was dropped onto a filter paper, which was then dried under an infrared lamp. The filter paper was then doubly sealed in polyethylene bags, and after irradiation, the outer bags were exchanged for new (non-irradiated) ones.

RESULTS: The contents of Cl, Br, and I in JCp-1 and JCt-1 were determined by RNAA and is shown in Table 1. Uncertainties refer to counting statistics (1σ) from gamma-ray spectrometry just after the radiochemical purification, as well as from those in the reactivation process. Information values for Cl have been reported as determined by spectrophotometry (584 and 95 mg kg^{-1} in JCp-1 and JCt-1, respectively) [8], which are in good agreement with the RNAA values from the present study, with uncertainties of 3σ. The estimates for the Br and I contents for these two carbonate materials are reported here for the first time. There is a scarcity of reliable and accurate halogen data for these materials. It is envisioned that the halogen data reported using RNAA will contribute to a compilation of such data for a database of GSJ/AIST reference materials.

Table 1 Cl, Br, and I contents in JCp-1 & JCt-1, as estimated by RNAA

Sample	Cl(mg kg^{-1})	Br(mg kg^{-1})	I (mg kg^{-1})
JCp-1	620 ± 27	3.22 ± 0.10	6.14 ± 0.15
JCt-1	103 ± 8	0.301 ± 0.011	0.031 ± 0.005

REFERENCES:

[1] MA Kndrick *et al.*, Geochim. Cosmochim. Acta **235** (2018) 285-304.
[2] L. Hughes *et al.*, Geochim. Cosmochim. Acta **243** (2018) 1-23.
[3] DE Harlov *et al.*, The Role of Halogens in Terrestrial and Extraterrestrial Geochemical Processes Springer Geochemistry, Gewerbestrasse, Switzerland (2018)
[4] S. Sekimoto *et al.*, Anal. Chem. **85** (2013) 6336-6341.
[5] S. Sekimoto *et al*., Geostand. Geoanal. Res. **41** (2017) 213-219.
[6] S. Aizawa, J. Radioanal. Nucl. Chem. **278** (2008) 349-352.
[7] M. Inoue *et al*., Geostand. Geoanal. Res. **28** (2004) 411-416.
[8] T. Okai *et al*., Chikyuukagaku **38** (2004) 281-286.
[9] B. Deruelle et al., Earth Planet. Sci. Lett. **108** (1992) 217–227.

CO5-21 Long term analysis of Cs isotopic ratio by thermal ionization mass spectrometry

Y. Shibahara, S. Fukutani and T. Kubota

Institute for Integrated Radiation and Nuclear Science, Kyoto University

INTRODUCTION: The applicability of the mass spectrometry has been studied for the analysis of radionuclide related to the nuclear incident such as the Fukushima Dai-ichi Nuclear Power plant accident. In the recent studies of our group, a thermal ionization mass spectrometer (TIMS) was applied for the analysis of Cs isotopic composition [1], and it was discussed that the analytical results of Cs isotopic composition obtained within the latest 2 financial years from April 2017 to March 2019 [2]. In this study, we discussed the additive agent used in the analysis of Cs isotopic composition by TIMS and the analytical results of Cs obtained within the latest 3 financial years from April 2017 to March 2020.

EXPERIMENTS: From the environmental sample obtained in Fukushima prefecture, Cs was recovered according to the recovery scheme discussed at the previous studies [3-5]. The concentration of ^{137}Cs of this sample corrected on Mar 11, 2011 was about 2.6×10^{-10} g/g. The Cs isotopic composition was analyzed by TIMS as the isotopic ratios of ^{134}Cs/^{137}Cs and ^{135}Cs/^{137}Cs.

A thermal ionization mass spectrometer (TRITON-T1, Thermo Fishier Scientific) was used for the analysis of Cs isotopic composition. The Cs sample was loaded onto a rhenium filament of a single filament system with a TaO activator or a glucose activator same as the previous study [2]. Because of the loading amount of Cs (*ca.* 1×10^{-12} g), the mass spectrometry was conducted with a secondary electron multiplier detector and the peak jump method [2-5]. For the discussion of the additive agent used to the ionization of Cs, about 1×10^{-12} g of the stable Cs (namely ^{133}Cs) was loaded onto a rhenium filament. TaO or glucose (or diluted them) was used as the additive agent.

RESULTS: Figure 1 shows the mass spectrum of Cs recovered from the environmental sample (observed at Oct 2019), and shows the peaks corresponding to ^{133}Cs, ^{134}Cs, ^{135}Cs and ^{137}Cs. It was observed that the ionization of Cs was affected by the kind of the additive agent, while that was not affected the dilution of additive agents with the dilution rate among 1 to 10.

The analytical result of ^{135}Cs/^{137}Cs ratio obtained within latest 3 years was shown in Fig. 2. The averaged value of 0.365±0.003 was obtained, and this value shows the good agreement with the previous study [2] (0.365±0.004). From the time profiles of ^{135}Cs/^{137}Cs and ^{134}Cs/^{137}Cs, the half-lives of ^{134}Cs and ^{137}Cs were evaluated as $T_{1/2(\mathrm{Cs\text{-}134})}$ = 2.07±0.03 y and $T_{1/2(\mathrm{Cs\text{-}137})}$ = 30.2±2.2 y respectively. These values also show the good agreement with the previous study [2] (2.08±0.02 y for ^{134}Cs and 30.2±2.2 for ^{137}Cs) and the literature data [6] (2.07 y for ^{134}Cs and 30.2 y for ^{137}Cs).

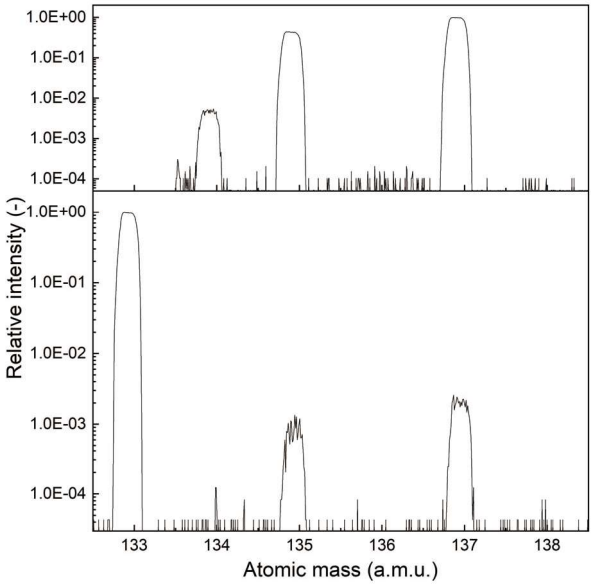

Fig. 1. Mass spectra of Cs recovered from environmental sample obtained at Fukushima prefecture observed at Oct 2019.

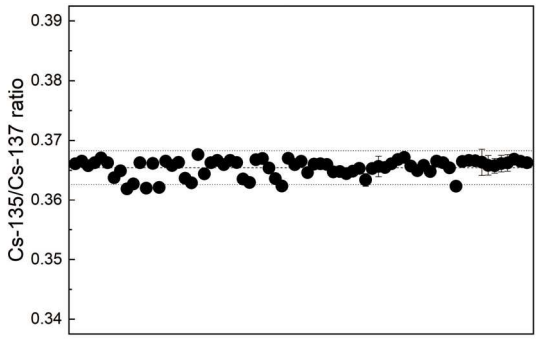

Fig 2. Results of Cs isotopic ratio analysis obtained within latest 3 years corrected on March 11, 2011.

REFERENCES:

[1] Y. Shibahara *et al.,* KURRI progress report 2017, 157.
[2] Y. Shibahara *et al.,* KURRI progress report 2018, 103
[3] Y. Shibahara *et al.,* J. Nucl. Sci. Technol. 2014, 51, 575-579.
[4] Y. Shibahara *et al.,* Radiological issues for Fukushima's revitalized future. Springer. 2016. 33-46.
[5] Y. Shibahara *et al.,* J. Nucl. Sci. Technol. 2017, 54, 158-166.
[6] R.B. Firestone *et al.,* Table of Isotopes, John Wiley and Sons, New York, 1998.

CO5-22 Analysis of Cd and As in the rice seed detected from the remains by NAA

T. Inamura, S. Fukutani[1] and K. Takamiya[1]

Archaeological Institute of Kashihara, Nara Prefecture
[1] Institute for Integrated Radiation and Nuclear Science, Kyoto University

INTRODUCTION: Parameters of the rice yield at the Yayoi period have been investigated on the basis of nitrogen supply, paddy structure etc. One of the important parameters to estimate the yield is the submerged condition of the paddy fields. However, the submerged condition has not been clear yet. It was found that the elemental composition of Cd and As of brown rice is good index of the submerged condition by elemental analysis using ICP-MS for modern rice seeds in the previous work [1]. However, the detected rice seeds which is cultural assets must be analyzed by a nondestructive method. We have tried to analyze the concentration of Cd and As of the detected rice seed by NAA (neutron activation analysis) using pneumatic irradiation system and normal Ge-detectors, and succeeded to determine the amount of As. On the other hand, the amount of Cd could not be estimated. The seeds buried in the ground contain high amounts of mineral elements compared to fresh seeds, and the mineral components such as iron and sodium disturb the determination of Cd by large Compton-background in gamma-ray measurements. In order to decrease the Compton continuum in gamma-ray measurement, determination of Cd using a Ge-detector combined with Compton suppression systemin had been tried in the previous work [2]. But the photo peak of Cd isotopes; ^{107}Cd ($t_{1/2}$ = 6.5 h), ^{111m}Cd ($t_{1/2}$ = 48.5 m) and ^{115}Cd ($t_{1/2}$ = 53.5 h), was not detected. In the present work, we irradiated rice samples using hydraulic irradiation system of KUR to detect the photo peaks of ^{109}Cd which has longer half-life of 462 d.

EXPERIMENTS: The buried rice seeds (Fig. 1) and chaffs irradiated in the present work were excavated at the Daifuku remains in Nara. The main elemental components of the samples were analyzed by EDX (Energy Dispersive X-ray spectrometry) before neutron irradiation. It was found that high amount of iron which produces long half-lived isotopes, ^{59}Fe ($t_{1/2}$ = 44.5 d), is contained in the rice samples. Several grams of the samples double-sealed with polyethylene bag and aluminum foil was encapsulated in an aluminum capsule. Neutron irradiation for the samples was performed using the hydraulic neutron irradiation system for 70 hours under 1 MW operation of KUR. After the irradiation, sample stands for three months to decrease activities of short-lived nuclides such as ^{56}Mn, ^{24}Na and also long-lived ones such as ^{59}Fe, ^{46}Sc ($t_{1/2}$ = 83.8d) produced by the neutron irradiation. The gamma-ray spectra of irradiated samples were measured by a Ge-detector to check the degree of disturbance caused by long-lived nuclides in the sample.

Fig. 1 The rice seeds sample excavated at the Daifuku remain.

RESULTS: The activity of ^{59}Fe decrease to about fourth compared with that at the end of irradiation. However, it was not low enough to detect photo peaks of ^{109}Cd clearly. The result suggests longer cooling time is required to decrease the activity of ^{59}Fe and detect photo peaks of ^{109}Cd. In the near future, the gamma-ray measurement will be carried out under the condition of low activities of ^{59}Fe and other products.

REFERENCES:

[1] T. Inamura *et al*., KURRI Progress Report 2017 (2018) 208-208.
[2] T. Inamura *et al*., KURRI Progress Report 2018 (2019) 189-189.

CO5-23 Ananysis method of strontium in seawater

Y. Ogata, H. Minowa[1], S. Kojima[2], Y. Kato[3] and K. Takamiya[4]

Nagoya University
[1]The Jikei University School of Medicine
[2]Aichi Medical University
[3]Hitachi, Ltd.
[4]Institute for Integrated Radiation and Nuclear Science, Kyoto University

INTRODUCTION: Conventional analysis methods of radiostrontium in seawater are complicated and time-consuming using a lot of deleterious substances. We are developing rapid and safe methods[1,2],. In the new method, strontium is collected on a filter with methods using ion exchange resin or Sr adsorbent, and is measured by a liquid scintillation counter using plastic scintillator. In this experiment, we tried to analyse behavior of Ba and Na through the procedure. First of all, ^{24}Na was measured with modified sum-peak method developed by Ogata[3, 4], also ^{46}Sc was measured to verify the method. After them, we analyse the behavior of Ba.

EXPERIMENTS: ^{24}Na produced by KUCA reactor was set on a p-type HPGe detector, GEM-35190S (ortec). The gamma spectrum from 0 to 4 MeV was converted to 8192 ch digital data with an ADC (Multi-port II, Canberra). The spectra were analysed using Gamma Explorer® software (Million Technologies). The source was placed on the axis of the detector at S–D distances (i.e., the distances from the surface of the end cap of the detector to the source), which were varied from 0 cm to 10 cm. The measurement time was set to collect more than 10,000 counts under the sum-peak area. Two peak counts, 1369 keV and 2754 keV, the sum peak counts and the total counts were collected. Also, ^{46}Sc produced by KUCA reactor was measured as the same way above. The peak, 889 keV and 1121 keV, the sum peak and the total counts were analysed. The angular correlation of the two peaks used here is 1.1184[5].

The behavior of Ba is trying to analysis. Radiobarium produced by KUCA reactor was add to seawater sample. Chemical separation procedure, using ion exchange or Sr adsorbent, was performed and radiobarium in each fraction was analysed.

RESULTS: Fig. 1 shows the results of the sum-peak method and the modified sum-peak method applied to ^{24}Na analysis. The abscissa is the count rate of 1389 keV peak and the ordinate is the estimated activity. The activities calculated with the sum-peak method and the modified sum-peak method were 2.83 kBq and 3.25 kBq, respectively. The activities were somewhat different from the activity calculated using efficiency at SDD 10 cm, 3.18 kBq, where the sum peak effect was negligible. However, no reliable figure of the angular correlation of the two peaks was available. Therefore, the results cannot be verified. Contrary, the results of ^{46}Sc are shown in Fig. 2. The calculated

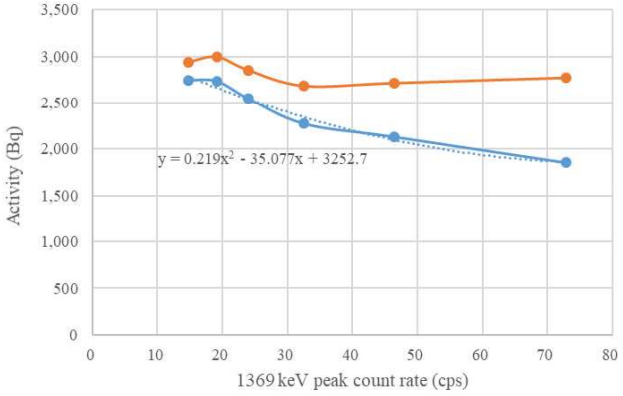

Fig. 1 ^{24}Na analysis with the sum-peak methods.

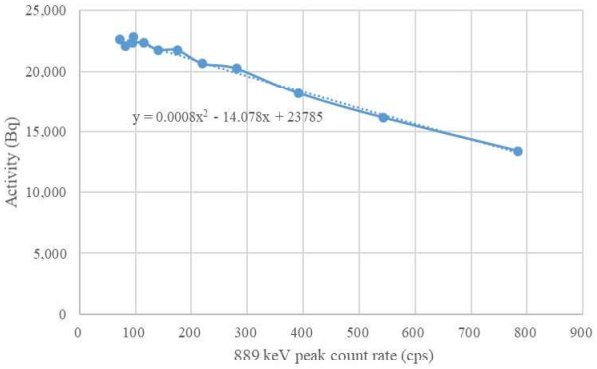

Fig. 2 ^{26}Sc analysis with the sum-peak methods.

activity by the modified sum-peak method were 26.6 kBq, and the figure was a little bit smaller than the activity calculated from the data obtained at SDD 10 cm, 28.7 kBq. The reason is now in investigation.

About the behavior of Ba, the limited results showed that Ba was remain in the filter for both procedures. Therefore, just after the reactor accident, ^{140}Ba was collected on the filter. But the half-life of ^{140}Ba is only 12.8 d, so that tree months after, the activity was less than two thousandth. Therefore, the effect would be limited. And the increase of the count brings conservative results. Moreover, the ^{140}Ba concentration will be estimated from the results by gamma spectroscopy by HPGe.

More detailed analysis will be performed hereafter.

[1] K. Yuka *et al.*, Proc. 19th Workshop on Environ. Radioact. KEK Proc. 2018-7, (2018).
[2] K. Yuka *et al.*, Proc. 33th Workshop on Environ. Radiation Uses. KEK Proc. 2019-4, (2019).
[3] Y. Ogata *et al.*, Nucl. Inst. Meth. Phys. Res. A. **775** (2015).
[4] Y. Ogata *et al.*, Appl. Radia. Isot., **109** (2016).
[5] G. Bertolini *et al.*, Nuovo Cimento, 3 (1956).

CO5-24

INAA using KUR for the determination of elemental content in air particulate samples

J.H. Moon, H.R. Lee, Y. Iinuma[1], H, Yoshinaga[1], R. Okumura[1], S. Fukutani[1]and K. Takamiya[1]

Neutron & RI Utilization Research Division, Korea Atomic Energy Research Institute, South Korea
[1]Institute for Integrated Radiation and Nuclear Science, Kyoto University

INTRODUCTION: Air quality in urban areas is one of the most important environmental issues and air particulates consisting of various elements from both artificial and natural origins is an indicator of an air quality. Especially, toxic elements in fine air particulates can be accumulated in the lungs by inhalation and incur serious harmful effects to human health. In this study, instrumental neutron activation analysis (INAA) was applied for the determination of the trace elements in air particulate samples collected from two different sampling sites in South Korea.

EXPERIMENTS: PM10 and PM2.5 air particulate samples were collected by using high volume samplers (HiVol 3000, Ecotech, Austria) and quartz filter (8 x 10 inches) in Seoul and Daejeon during the spring season, 2019. Sixty-eight analytical samples (17 samples for PM10 and PM2.5 at Seoul and Daejeon) with size of 15 x 223 mm were prepared and NAA facilities at KUR were employed for INAA, because of shut-down of HANARO research reactor in Korea. The prepared samples were irradiated using the PN3 irradiation hole for 2 minutes to detect short-lived nuclides at 1 MW and for 50 minutes to detect medium/long-lived nuclides at 5 MW, respectively. Thermal neutron flux was measured by using Al wire for short irradiation and Fe wire for long irradiation. After proper decay according to target nuclides, gamma-rays emitted from the irradiated samples were measured by using gamma-ray spectrometer with a high purity Ge detector. Elemental contents were determined by activation formula based on absolute quantification method [1, 2]. Four blank filters were analyzed under the same analytical condition with particulate samples.

Fig. 1. A photo of PM10 and PM2.5 samplers in Daejeon.

RESULTS: Twenty-four elements like Al, Ba, Br, Ce, Co, Cr, Dy, Eu, Fe, Hf, K, La, Mg, Mo, Mn, Na, Sb, Sc, Sm, Tb, Th, U, Yb, Zn, were detected and quantified from blank filter samples. Among them, Al content is not confident, due to the fast neutron reaction of Si (main matrix of filter media). As, Au, Cl, I, In, Se, V and W were additionally determined in the air particulate samples. Eventually, thirty-two elements can be determined from the actual samples by INAA. The concentrations (ng/m^3) of ten toxic elements such as As, Ba, Br, Cl, Cr, Fe, Mn, Sb, V and Zn of 32 elements were calculated with air flow volume and by the subtraction of elemental contents in blank filter, and their average concentrations were evaluated for 17 samples. The results are shown in Table 1. As expected, most of elemental concentrations in Seoul samples were higher than those in Daejeon samples, except for Cl. Fe shows the highest concentration level (0.81 ~ 2.19 μg/m3) among ten toxic elements, and As, Sb and V have a similar concentration level (2 ~ 10 ng/m3). These results will be used for various purposes such as epidemiological studies, source identification and apportionment [3].

Table 1. Concentration results for 10 toxic elements

Element	Seoul PM10	Seoul PM2.5	Daejeon PM10	Daejeon PM2.5
As	5.15±3.50	4.78±3.13	6.38±6.22	4.80±3.42
Ba	68.6±31.4	42.9±26.3	19.8±7.50	17.2±6.77
Br	18.9±22.0	19.7±24.3	17.1±5.66	15.4±5.59
Cl	352±194	334±204	916±595	515±275
Cr	10.5±4.91	8.68±4.03	6.39±2.16	5.62±1.40
Fe	2190±1370	1650±1120	1140±606	809±514
Mn	43.9±27.5	39.8±27.3	32.5±14.6	28.0±13.1
Sb	9.03±7.71	6.95±7.22	3.14±1.67	2.72±1.42
V	8.27±5.54	8.43±6.14	5.84±3.42	5.60±3.24
Zn	115±72.1	103±63.9	88.5±47.0	71.5±36.2

REFERENCES:

[1] D. De Soete, R. Gijbels, J. Hoste, Neutron Activation Analysis, Wiley-Interscience, New York (1972).
[2] R.R. Greenberg, P. Bode, E.A. De Nadai Fernandes, Neutron activation analysis: a primary method of measurement, Spectrochim. Acta Part B 66 (2011) 193–241.
[3] J. M. Lim, J. H. Lee, J. H. Moon, Y. S. Chung, K. H. Kim, Source apportionment of PM10 at a small industrial area using Positive Matrix Factorization, Atmospheric Research 95 (2010) 88–100.

31169, 31170